Vol. 13, No. 1, pp. 13-21 (2013)
Journal of Agricultural Physics
ISSN 0973-032X
http://www.agrophysics.in

Research Article

Loss of Soil Carbon and Nitrogen through Wind Erosion in the Indian Thar Desert

PRIYABRATA SANTRA*[1], R.S. MERTIA[2], R.N. KUMAWAT[3], N.K. SINHA[2] AND H.R. MAHLA[2]

[1]*Central Arid Zone Research Institute, Jodhpur-342003, Rajasthan*

[2]*Central Arid Zone Research Institute, RRS, Jaisalmer-345001, Rajasthan*

[3]*Zonal Project Directorate (Zone-VI), CAZRI campus, Jodhpur-342005, Rajasthan*

ABSTRACT

Wind erosion is the most noticeable land degradation process in the hot arid region of India that covers about 16% of the geographical area of India. It results into loss of considerable amount of nutrient-rich particles from the region. Field investigations were carried out in a rangeland site located at Jaisalmer centre of Central Arid Zone Research Institute in the province of western Rajasthan to quantify the nutrient loss through wind erosion. The aeolian mass fluxes (M L^{-2} T^{-1}) were collected at four different heights: 0.25 m, 0.50 m, 0.75 m, and 2 m above land surface. Analysis of eroded soil was performed using Foss Heraeus CHN-O-rapid elemental analyzer. The results have revealed an average loss of 4 g C kg^{-1} and 0.37 g N kg^{-1}. Present study shows that the C and N content in eroded soils were highest during the month of July and the accumulated annual loss was approximated as 45.9 kg C ha^{-1} and 4.3 kg N ha^{-1}. To mitigate such appreciable soil nutrient losses through wind erosion, suitable rangeland utilization practices, which can help to retain the soil health and would also support the crop/grassland productivity in arid ecosystem, need to be evolved on priority.

Key words: Dust storm, Carbon and nitrogen loss, Desert rangelands, Wind erosion

Introduction

Desertification is affecting the livelihoods of more than 2 billion people across the world living in dryland areas that occupy nearly 41% of the Earth's land area. In India, about 22.96 m ha land is affected by desertification, out of which 15.2 m ha land is affected by wind erosion (Kar *et al.*, 2009). During wind erosion events, considerable amount of nutrient rich soil particles are eroded from top soil surface in the Indian Thar desert (Santra *et al.*, 2006, Mertia *et al.*, 2010). Loss of topsoil from arable desert soils consequently leads to the loss of soil productivity (Larney *et al.*, 1998; Zhao *et al.*, 2006a). These nutrient-rich aeolian masses may also travel long distances along with supra-regional dust storms influencing ecosystems that are far away from the origin of these dust particles (Zhao *et al.*, 2006b, Hoffman *et al.*, 2008). Deposition of such aeolian sediments is also considered to have important fertilizing effect on grasslands in the arid and semi-arid regions, field boundaries, surface water bodies, etc. (Offer *et al.*, 1996).

*Corresponding author,
Email: priyabrata.iitkgp@gmail.com

Abbreviations: CHN-O: Carbon Hydrogen Nitrogen-Oxygen; SOC: Soil Organic Carbon; DSE: Dust Storm Event; POWE: Periodical Observations on Wind Erosion

Loss of topsoil influences soil organic carbon (SOC) and nitrogen dynamics (Mendez *et al.*, 2006) that eventually affect the soil carbon sequestration potentials (Stallard, 1998; Lal, 2003). Conservation and maintenance of SOC contents is a key step in maintaining soil quality and productivity. Progressive trends of landuse changes from natural rangeland ecosystem to arable farming in dryland areas have also resulted in faster decline of the meager SOC pool of desert soils and even more under the scenario of global climate change related desertification processes (Lal, 2001; Dawson and Smith, 2007). Investigation on quantification of carbon (C) and nitrogen (N) losses through wind erosion may help to assess the adverse environmental impacts in desert regions. Several studies on Indian deserts (Dhir, 1985; Narain *et al.*, 2000) revealed the richness of eroded soils in terms of nutrient contents. However, these studies were confined to surface deposited sediments only. However, reports are sparse on the quantification of C and N losses through field investigations and their periodical variations. Therefore, the present field investigation was carried out to assess the C and N losses through suspended soil sediments due to continuous wind erosion and dust storm events in the Indian Thar desert.

Material and methods

Study site

Field investigation on wind erosion / dust storm events was carried out in a rangeland site, which was located at 6 km eastward from Jaisalmer city in the Indian Thar desert (Fig. 1). The site was dominated with *Lasuirus sindicus* (sewan) grass, an abundantly available perennial plant species in the Indian Thar desert. Tussock density of sewan grass at the site was 8000-9000 tussocks ha^{-1}. Grazing of animals in the field site was regulated through fencing and by allowing

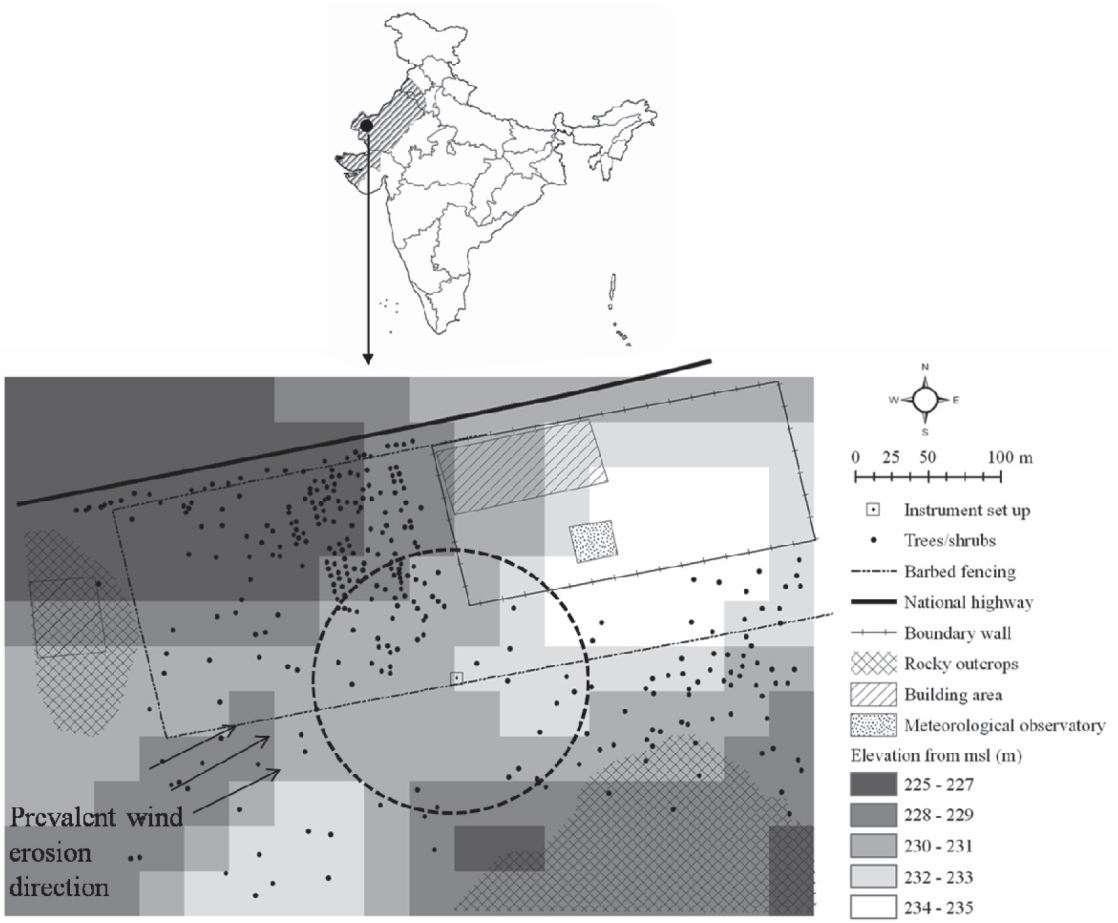

Fig. 1. Location of field experimental site at Jaisalmer region of the Indian Thar desert

cattle to browse up to 70% of available biomass leaving behind a grass height of 10-15 cm from surface. Bushes of *Ziziphus mauritiana*, *Propospis juliflora*, *Calotropis procera*, *Aerva persica* etc., with maximum canopy height of 3 m were sparsely available at the site with an average density of 15 bushes ha^{-1}. Soils were shallow in depth (60-70 cm) with occurrence of calcite concretion below the soil profile in most cases. Soils of the region were predominantly classified as Typic Torripsamments (Shyampura *et al.*, 2002).

Meteorological data

Daily data on meteorological parameters during field investigation period from June to September of the year 2009 are presented in Fig. 2. Annual rainfall during the study year was 73.6 mm, which was far less than the long term average of the region (196 mm). Maximum and minimum air temperatures during field investigation were 33-46°C and 20-30°C, respectively. Daily average relative humidity was 58.6%. Daily average wind speed ranged between

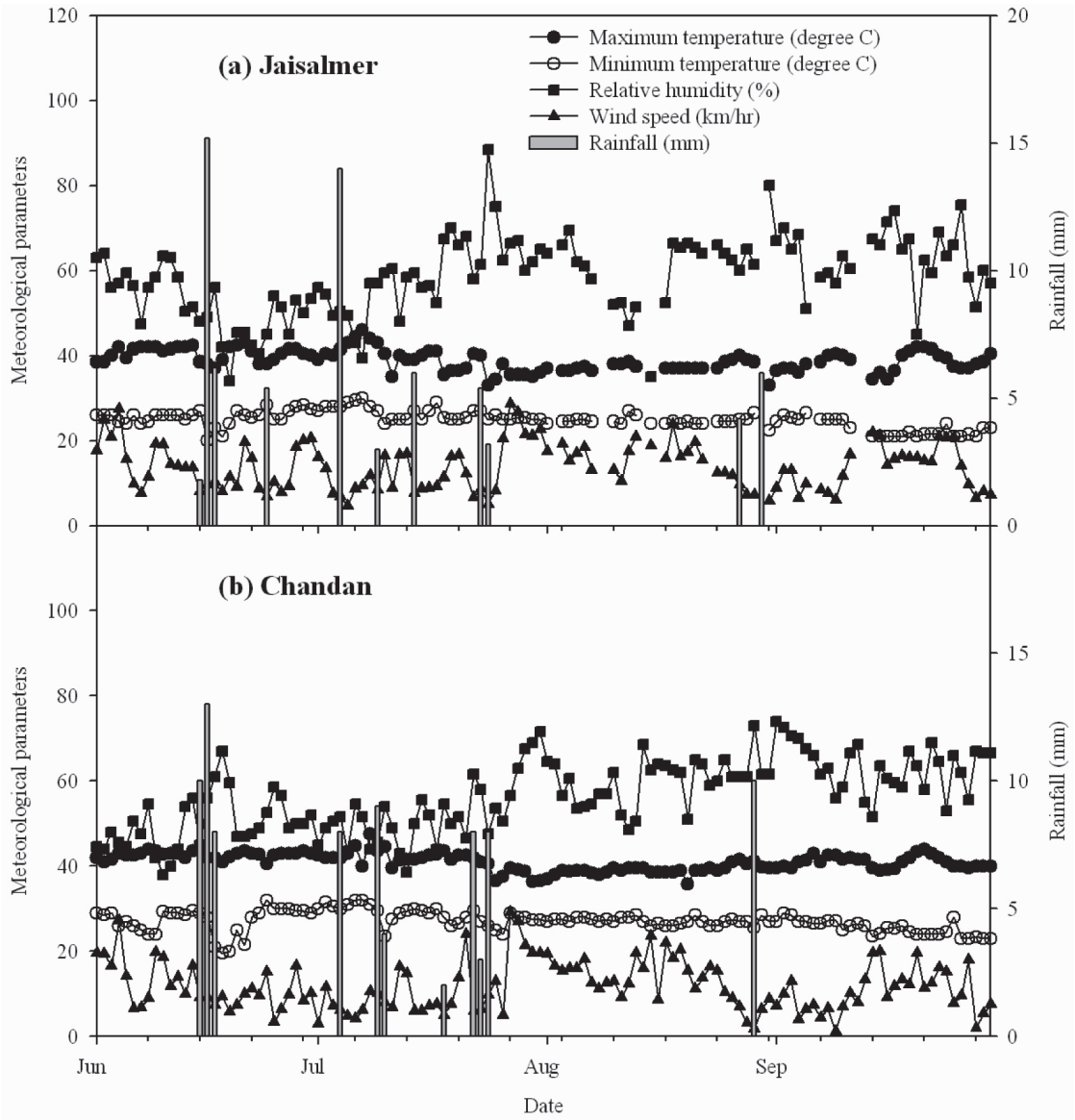

Fig. 2. Mean daily meteorological parameters during the observation periods (June-September, 2009) at the experimental site located at Jaisalmer, Rajasthan, India

4.58 and 28.62 km hr^{-1} with an average of 13.84 km hr^{-1}.

Measurements on loss of soil carbon and nitrogen through wind erosion

For the present field investigation, wind erosion sampler designed and fabricated by Santra *et al.* (2010) was used to collect wind eroded aeolian masses during wind erosion / dust storm events. The collection efficiency of the sampler was 85-90%. The sampler with four collectors at different heights from surface was installed at the center of the field site. The approximate distance between the sampler and surrounding non-eroding boundaries at the periphery of the field site ranged from 100 to 200 m. Rocky outcrops on western side, barbed wire fences inhabiting scattered trees of about 2-3 m height on northern and north western side, concrete boundary wall of about 1.5 m height on north eastern side and again rocky outcrops on south eastern side represented the non-eroding periphery of the field site (Fig. 1a). Apart from these, a long fetch of land with scattered grasses and shrubs on south western side and a small hillock at 500-600 m distance from the sampler on the south western side were present.

Four collectors of the sampler were fixed at 0.25, 0.75, 1.25, and 2 m height from land surface. Polyethylene bags were fixed at the end of the collector to store the entrapped soil mass inside the collector. Wind eroded soil masses were emptied from polyethylene bags and carried to the laboratory either at fortnight interval or after the occurrence of dust storm event. Eroded amount of soil mass for each sampling height was then converted into mass flux (M L^{-2} T^{-1}). Calculated mass fluxes were multiplied with a correction factor of 1.176 considering the average efficiency of the sampler as 85%. Mass-fluxes of eroded aeolian masses were fitted in power decay mass-height profile model, which was considered as the best model for the Indian Thar desert (Mertia *et al.*, 2010) and is shown in Eq (1):

$$q(z) = a z^{b} \quad \ldots(1)$$

where, q is the mass flux (M L^{-2} T^{-1}) of wind eroded soil at height z (L) from surface; 'a' and 'b' are empirical constant of the equation. Total aeolian mass transport rate (M L^{-1} T^{-1}) was computed through integration of Eq (1) with lower limit of z = 0.25 m to upper limit of z = 2 m representing the suspension mode of wind erosion. However, to calculate the approximate estimate of total soil loss, lower limit of z was extrapolated up to 0.01 m height from land surface. The calculated mass transport rate was converted into soil loss (M L^{-2}) for each observation period by approximating the average width of experimental field site as 150 m.

C and N content of each collected sample were analyzed using Foss Heraeus CHN-O-rapid elemental analyzer. The variation in C and N content of eroded soil with height from surface and time of the season were analysed using Tukey's multiple comparison tests. Total loss of C and N due to wind erosion were computed as follows:

Total C/N loss (kg ha^{-1}) = C/N content of eroded soil (g kg^{-1}) × soil loss (kg ha^{-1}) …(2)

Results and Discussion

Soil loss due to wind erosion

A total of five dust storm events (DSE) and five periodical observations on wind erosion events (POWE) were recorded during the investigation period from June to September, 2009 (Table 1). The wind erosion sampler collected significant amount of eroded masses during both DSE and POWE. After the month of September, although few scattered POWE were observed but they were very weak to cause any significant soil loss and hence are not included in Table 1. Computed soil loss through suspension mode during DSE revealed a maximum soil loss of 389 kg ha^{-1} during a single dust storm event on June 15, 2009 (DSE-1), which prevailed for about 30 minutes duration (Table 1). Cumulative soil loss through suspension mode during the middle of June till the end of September of the year 2009 was 1.36 t ha^{-1} whereas extrapolating the Eq (1) very near to surface (lower limit of z = 0.01 m) resulted into a total soil loss of 12.02 t ha^{-1}. It was also noticed that almost half of the total soil

Table 1. Wind erosion / dust storm events during June to September, 2009 at Jaisalmer and the approximate soil loss during each event

Name of the observations	Time of occurrence	Duration	§Soil loss in suspension mode (kg ha^{-1})	§§Total soil loss (kg ha^{-1})
Dust storm events (DSE)				
DSE-1	June 15, 2009	30 min	389	1166
DSE-2	June 17, 2009	20 min	246	466
DSE-3	June 24, 2009	15 min	19	58
DSE-4	July 09, 2009	25 min	128	1485
DSE-5	July 14, 2009	15 min	16	30
Periodical observations on wind erosion (POWE)				
POWE-1	June 25 – July 2, 2009	7 days	23	30
POWE-2	July 15 – July 30, 2009	16 days	203	3244
POWE-3	July 31 – Aug 18, 2009	19 days	255	5287
POWE-4	Aug 19 – Sept 3, 2009	15 days	49	68
POWE-5	Sept 4 – Sept 23, 2009	20 days	39	188

§Soil loss was computed within the observation heights (0.25 to 2 m above surface), which generally indicates the soil loss in suspension mode

§§Total soil loss was calculated through extrapolation of mass-height profile up to very near to soil surface (0.01 m)

loss was occurred through dust storm events and rest half during local wind erosion events. Average rate of soil loss was observed as 17 kg ha^{-1} min^{-1} during DSE and 25 kg ha^{-1} day^{-1} during POWE.

Carbon and nitrogen loss through wind erosion

Average C and N content of eroded soils from the experimental site were 4 g kg^{-1} and 0.37 g kg^{-1}, respectively with a range of 3.01-5.44 g kg^{-1} C and 0.30-0.51 g kg^{-1} N. In general, both C and N contents were higher during DSE as compared to POWE. It was also observed that average C and N contents of surrounding top soils at the field site were 5.01 g kg^{-1} C and 0.44 g kg^{-1} N, respectively, in spite of the loss of almost similar amount through wind erosion processes. It indicates the gain of C and N at experimental site through simultaneously occurring deposition processes, which was not directly measured in the present study. However, nutrient enrichment through dust deposition in the field site can be approximated indirectly from several measured data on C content in the region. For example, average soil organic carbon (SOC) content of 78 soil samples covering eight land use systems at Jaisalmer region was observed < 2 g kg^{-1}. Similarly, SOC content of 117 soil samples in a cultivated farm of 76 ha at Jaisalmer region was observed to range from 1.06 to 2.13 g kg^{-1} (Santra *et al.*, 2012). From these two databases, overall SOC content from Jaisalmer region may be considered < 2 g kg^{-1}. With the application of suitable conversion factor (Krishnan *et al.*, 2009), the average C content of Jaisalmer as per CHN-O analyser may be approximated as < 3 g kg^{-1}. Carbon content of the top soil at the field site was found slightly higher (5.01g kg^{-1}) than the average C content of soils in Jaisalmer region (~ 3 g kg^{-1}). Therefore, we consider overall enrichment of soils in the rangeland site based on the above measurements and approximations. Moreover, average C content of eroded soil (4 g kg^{-1}) was found to be lower than parent soil (5.01 g kg^{-1}). It indicates that apart from dust emission, deposition of eroded soil mass in rangeland is common, which finally leads to enrichment of top soils. However, continuous overgrazing associated with severe drought situations in the desert may lead to rapid loss of these top fertile soils.

Table 2. Carbon (C) and Nitrogen (N) contents of eroded soils at different sampling heights during wind erosion events at Jaisalmer

Sampling heights	§C (g kg^{-1})		§N (g kg^{-1})	
	DSE	POWE	DSE	POWE
0.25 m	4.25±0.30	3.97±0.52	0.40±0.03	0.34±0.02
0.75 m	4.51±0.33	3.50±0.20	0.42±0.04	0.34±0.02
1.25 m	4.38±0.40	3.47±0.13	0.42±0.05	0.33±0.02
2.00 m	4.40±0.53	3.44±0.41	0.40±0.04	0.34±0.03
Topsoil	5.01±0.18	0.44±0.03		

§Values of C and N content are not significantly different between heights of observations (P<0.05, Tukey test).

Height wise variation in C and N contents

Average C and N content of the eroded soils at different sampling heights above land surface is presented in Table 2. It was observed that the C and N content of eroded soil did not significantly vary with height both during DSE and POWE ($p<0.05$). Initially, we hypothesized that C content in eroded soils would increase with height as C particles were lighter than mineral soils but no such significant trend was observed in the present study. However, slight increase in C and N content of eroded soil with sampling height was observed during severe wind erosion events. For example, during DSE-4 occurred on July 9, 2009, C content increased with height from 4.73 g kg^{-1} at the sampling height of 0.25 m from surface to 5.44 g kg^{-1} at the sampling height of 2 m from surface. Similarly, N content of eroded soils during DSE-1 occurred on June 15, 2009 increased from 0.34 g kg^{-1} at 0.25 m height to 0.48 g kg^{-1} at 2 m from surface. Similar to these observations, Hoffman *et al.* (2008) also reported non significant variation in C and N content in eroded soil with height from land surface except in case of severe wind erosion events, for which about 10% and 24% increase in C and N content, respectively, was reported with an increase in height from near land surface to 1 m above land surface. Observed C and N contents in eroded soil masses as reported by Hoffman *et al.* (2008) varied from 29-47 g kg^{-1} of C and 2.7-4.2 g kg^{-1} of N, which was quite higher than C and N loss in the present study (3.01 to 5.44 g kg^{-1} C and 0.30 to 0.51 g kg^{-1} N). However, Bielders *et al.* (2002) reported the loss of 0.2-0.3 g N kg^{-1} through wind erosion in Sahel region, which was slightly lower than the observed values from the present investigation.

Periodical variation

Variation of C and N contents of eroded soils with time for the season is presented in Fig. 3. Carbon content of eroded soils was observed maximum (5.13 g kg^{-1}) during DSE-4 at the second week of July and reduced to the minimum of 3.35 g kg^{-1} at the end of September. Similarly, N content of eroded soils was also observed maximum (0.50 g kg^{-1}) during DSE-4 at the second week of July and reduced to the minimum of 0.33 g kg^{-1} at the end of September. Month-wise comparison has revealed that during July, both C and N contents were significantly higher than other periods of the year. Higher C and N content in eroded soil during July was probably due to exposure of soils underneath top thin layer of relatively coarse sand particles, which was eventually removed during few initial wind erosion events at the beginning of summer season.

Total loss of C and N

Cumulative loss of soil nutrients along with the eroded mass during three and half month's period from the middle of June to the end of September was calculated as 45.93 kg C ha^{-1} and 4.37 kg N ha^{-1}. Among dust storm events, the highest loss of C was recorded during DSE-1 and the associated loss was 4.39 kg C ha^{-1}. Among periodical observations, the loss of C was highest during POWE-3 and the corresponding loss was 17.73 kg C ha^{1}. The average nutrient loss was

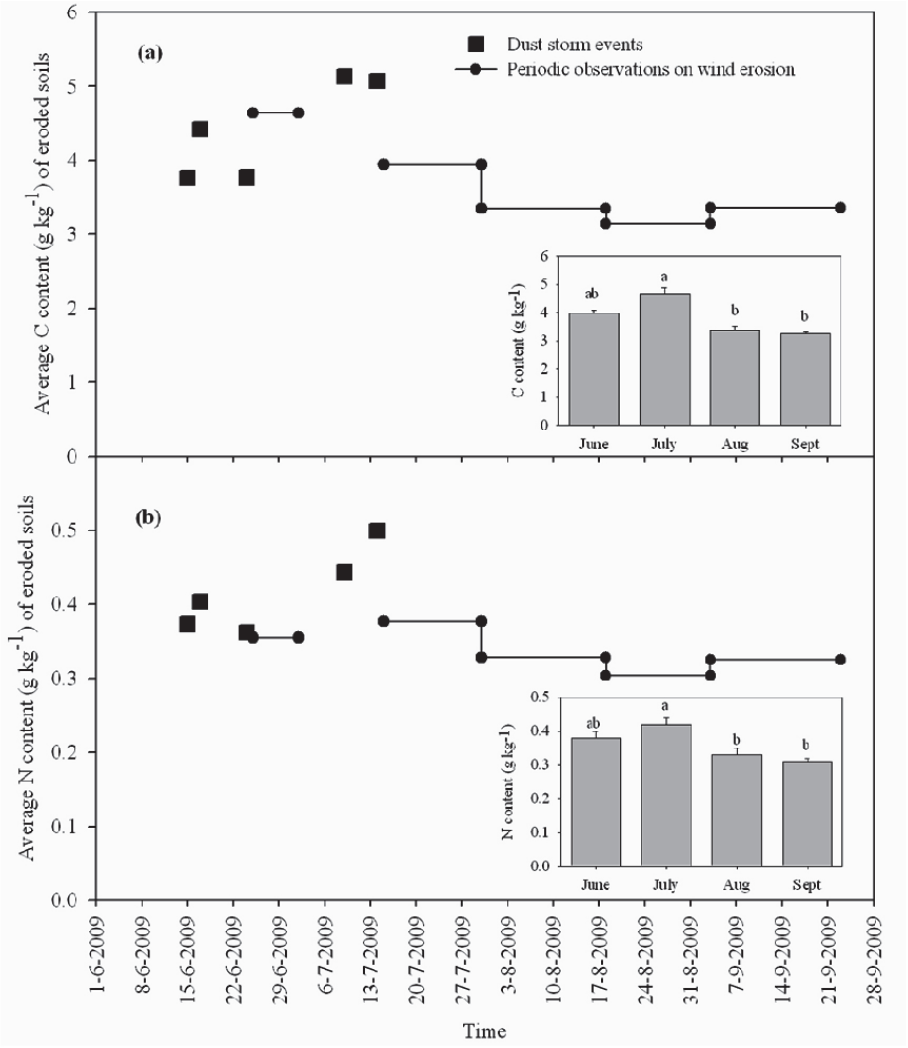

Fig. 3. Periodic variation of carbon (C) and nitrogen (N) content of eroded soils; (a) C content and (b) N content Values with the same letters above the bars are not significantly different ($P<0.05$, Tukey test).

0.12 kg C ha^{-1} min^{-1} during DSE and 0.36 kg C ha^{-1} day^{-1} during POWE. Similarly, the loss of N was highest during DSE-1 and the associated loss was 0.44 kg N ha^{-1}. Among periodical observations, the loss of N was highest during POWE-3 and the associated loss was 1.73 kg N ha^{1}. It is notable here that the reported loss of C and N in this study was measured at a controlled grazing rangeland site. Therefore, the observed losses of C and N may be considered as the loss from semi-protected rangelands in the Indian Thar desert. Such loss of C and N from cultivated lands, open grazing rangelands and denuded soil surface are expected to be 3-5 times higher than these observed losses (Mertia *et al.*, 2010).

Conclusions

Measurements of wind eroded soil loss from a rangeland site at Jaisalmer region of the Indian Thar desert revealed significant loss of C and N through wind erosion processes. Average C and N contents in eroded soils was observed as 4 g C kg^{-1} and 0.77 g N kg^{-1}, respectively. Cumulative loss of C and N for a period of three and half months from the middle of June to the end of September was 46 kg C ha^{-1} and 4 kg N ha^{-1}. The present investigation was carried out at a controlled grazing rangeland site at Jaisalmer with a single measurement system and for a period of three and half months during summer season with

an attempt to analyze the impact of wind erosion on loss of C and N from rangeland ecosystem in the Indian Thar desert. A large part of the Indian Thar desert lies under similar type of rangelands, however with excessive grazing pressure. Therefore, the amount of soil loss and associated C and N loss from overgrazed rangeland is expected to be higher and has been reported by Mertia *et al.* (2010). Recently, several studies revealed a rapid conversion of rangelands into cultivable lands, which might have aggravated the problem of C and N loss through wind erosion. Therefore, temporal varation with intensive experimental set up may be initiated in different land use system of the Indian Thar desert focusing agricultural lands, overgrazed rangelands, rocky terrains, open sand dunes etc for overall assessment of C and N loss from the Indian Thar desert.

Acknowledgement

We sincerely thank the Director, Central Arid Zone Research Institute, Jodhpur for providing necessary supports and facilities to carry out the field investigations. We also sincerely thank the Director, Vivekananda Parvitya Krishi Anusandhan Shala (VPKAS), Almora, India for providing the CHN-O-rapid analyser facilities to determine carbon and nitrogen content of wind eroded aeolian samples.

References

Bielders, C.L., Rajot, J.L. and Amadou, M. 2002. Transport of soil and nutrients by wind in bush fallow land and traditionally managed cultivated fields in the Sahel. *Geoderma* **109**: 19-39.

Dawson, J.C. and Smith, P. 2007. Carbon losses from soil and its consequences for land use management. *Science of the Total Environment* **382**: 165-190.

Dhir, R.P. 1985. Characterization and properties of dune and associated soils. p. 41-49. In *Sand dune stabilization, shelterbelts and afforestation in dry zones*. Food and Agricultural Organization of the United Nations, Rome.

Hoffmann, C., Funk, R., Li, Y. and Sommer, M. 2008. Effect of grazing on wind driven carbon and nitrogen ratios in the grasslands of Inner Mongolia. *Catena* **75**: 182-190.

Kar, A., Moharana, P.C., Raina, P., Kumar, M., Soni, M.L., Santra, P., Ajai, Arya, A.S. and Dhinwa, P.S. 2009. Desertificatiion and its control measures. p. 1-47. In Kar, A., Garg, B.K., Singh, M.P. and Kathju, S. (Eds.), *Trends in Arid Zone Research in India*. Central Arid Zone Research Institute, Jodhpur, India.

Krishnan, G., Srivastava, S.K., Kumar, S., Saha, S.K. and Dadhwal, V.K. 2009. Quantifying the underestimation of soil organic carbon by the Walkley and Black technique-examples from Himalayan and Central Indian soils. *Current Science* **96**(8): 1133-1136.

Lal, R. 2001. Potential of desertification control to sequester carbon and mitigate the greenhouse effect. *Climate Change* **51**: 35-72.

Lal, R., 2003. Soil erosion and the global carbon budget. *Environment International* **29**: 437-450.

Larney, F.J., Bullock, M.S., Janzen, H.H., Ellert, B.H. and Olson, E.C.S. 1998. Wind erosion effects on nutrient redistribution and soil productivity. *Journal of Soil and Water Conservation* **53**: 133-140.

Mendez, M.J., Oro, L.D., Panebianco, J.E., Colazo, J.C. and Buschiazzo, D.E. 2006. Organic carbon and nitrogen in soils of semiarid Argentina. *Journal of Soil and Water Conservation* **61**: 230-235.

Mertia, R.S., Santra, P., Kandpal, B.K. and Prasad, R. 2010. Mass-height profile and total mass transport of wind eroded aeolian sediments from rangelands of Indian Thar desert. *Aeolian Research* **2**: 135-142.

Narain, P., Kar, A., Ram, B., Joshi, D.C. and Singh, R.S. 2000. *Wind erosion in Western Rajasthan*. CAZRI, Jodhpur, India.

Offer, Z.Y., Sarig, S. and Steinberger, Y. 1996. Dynamics of nitrogen and carbon content of aeolian dry deposition in an arid region. *Arid Soil Research and Rehabilitation* **10**: 193-199.

Santra, P., Mertia, R.S. and Narain, P. 2006. Land degradation through wind erosion in Thar Desert - Issues and Research priorities. Indian Journal of Soil Conservation **34**(3): 214-220.

Santra, P., Mertia, R.S. and Kushawa, H.L. 2010. A new wind erosion sampler for monitoring dust storm events in the Indian Thar desert. *Current Science* **99**(8): 1061-1067.

Santra, P., Kumawat, R.N., Mertia, R.S., Mahla, H.R. and Sinha, N.K. 2012. Spatial varation of soil organic carbon stock in a typical agricultural farm of hot arid ecosystem of India. *Current Science* **102**(9): 1303-1309.

Shyampura, R. L., Singh, S.K., Singh, R.S., Jain, B.L. and Gajbhiye, K.S. 2002. *Soil series of Rajasthan*. NBSS & LUP Publication No. 95, NBSS&LUP, Nagpur.

Stallard, R.F. 1998. Terrestrial sedimentation and the carbon cycle: coupling weathering and erosion to carbon burial. *Global Biogeochemical Cycles* **12**: 231-257.

Zhao, H.L., Yi, X.Y., Zhou, R.L., Zhao, X.Y., Zhang, T.H. and Drake, S. 2006a. Wind erosion and sand accumulation effects on soil properties in Horqin Sandy Farmland, Inner Mongolia. *Catena* **65**: 71-79.

Zhao, T.L., Gong, S.L., Zhang, X.Y., Blanchet, J.P., McKendry, I.G. and Zhou, Z.J. 2006b. A simulated climatology of Asian dust aerosol and its trans-Pacific transport. Part I: mean climate and validation. *Journal of Climate* **19**: 88-103.

Received: 2 December 2012; Accepted: 8 March 2013

HYDROLOGICAL PROCESSES
Hydrol. Process. **28**, 969–979 (2014)
Published online 17 December 2012 in Wiley Online Library
(wileyonlinelibrary.com) DOI: 10.1002/hyp.9631

Characterization of suspended sediment in Meltwater from Glaciers of Garhwal Himalaya

Deepak Srivastava,[1] Amit Kumar,[1]* Akshaya Verma[1] and Siddharth Swaroop[2]

[1] *Centre for Glaciology, Wadia Institute of Himalayan Geology, 33, GMS Road, Dehra Dun 248 001, Uttarakhand, India*
[2] *Geological Survey of India, GSI Complex, Vasundhara, Sector-E, Aliganj Lucknow 226024, Uttar Pradesh, India*

Abstract:

Glacierised basins are significant sources of sediments generated by glacial retreat. Estimation of suspended sediment transfer from glacierised basins is very important in reservoir planning for hydropower projects in Himalaya. The present study indicates that storage and release of sediment in proglacial streams may categorise the pattern of suspended sediment transfer from these basins. Assessment of suspended sediment concentration (SSC), suspended sediment load (SSL) and yield has been undertaken for Dunagiri Glacier basin located in Garhwal Himalaya (30°33'20"N, 79°53'36"E), and its results are compared with the Gangotri and Dokriani glaciers sharing close proximity. Out of the total drainage basin area, about 14.3 % of the area is glacierised. Data were collected for five ablation seasons (1984–1989, barring 1986). The mean daily SSCs for July, August and September were 333.9, 286.0 and 147.15 mg/l, respectively, indicating highest concentration of mean daily suspended sediment in July followed by August. SSL trends were estimated to be 93.0, 57.0 and 21.3 tonnes. About 59% of the total SSL of the melt period was transported during the months of August and September. Sediment yield for the study basin was computed to be 296.3 t km^{-2} yr^{-1}. It is observed that the cumulative proportion of SSC precedes the discharge throughout the melt season except in the year 1987. Release of SSL in terms of total load is less in the early part of melt season than in the later stage as compared to that of discharge. Diurnal variations in SSC reach their maximum at 2400 h, and therefore, SSC was found to be high during night (2000–0400 h). There was a good relationship between SSC and SSL with discharge for the ablation seasons (1988 and 1989). Mean monthly SSC and mean monthly SSL provide a good exponentional relationship with mean monthly temperature. Copyright © 2012 John Wiley & Sons, Ltd.

KEY WORDS suspended sediment; sediment yield; Himalaya; glacierised basins

Received 31 January 2012; Accepted 16 October 2012

INTRODUCTION

The analysis of sediments in fluvial systems and processes of sediment transport is receiving increasing attention all over the world among hydrologists, geologists and geomorphologists (Collins, 1979; Milliman and Meade, 1983; Hodgkins, 1996; Willis *et al*., 1996; Hodson and Ferguson, 1999; Syvitski, 2003; Walling and Fang, 2003; Lenzi *et al*., 2006; Schmidt and Morch, 2006; Wenfeng and Kateb, 2011). Suspended sediment studies have acquired great significance in present times, as effective working of power projects depend on the proper assessment of hydroelectric potential and suspended sediment yield transported by the glacial streams, which may prove detrimental to the reservoirs and turbines (Ostrem, 1975). Suspended sediment concentrations (SSCs) are controlled by composite interaction between sediment delivery and hydrological connectivity between the sediment source and the stream channel. Glaciers are major erosional agents, and therefore, important sources of suspended sediments (Collins, 1998).

In general, sediment transfer studies are done near the snout (terminus) of the glacier to compensate for the effect of runoff and the sediment source from the valley side of the basin. Specific sediment yield and sediment load generated by glacierised basins are always greater than that of non-glaciated basins (Jansson, 1988; Harbor and Warburton, 1993; Iverson, 1995; Hallet *et al*., 1996; Singh *et al*., 2003), because of the high sediment production due to glacier motion (Gurnell, 1995; Alley *et al*., 1997). Gurnell *et al*. (1994) compared the discharge and suspended sediment transport of an arctic glacier and an alpine glacier, which were of similar size, and reported strong diurnal variations in the SSC in the alpine proglacial river than in the arctic environment. Higher SSC occurred after the majority of snow in the basin was melted and was preceded by a long period of relatively high air temperature in the arctic region (Lewis *et al*., 2005). Hydrological characteristics of the subglacial and englacial drainage system in Gulkhana Glacier, Canada show that the event of rapidly increasing discharge and sediment load is due to the collapse of the subglacial drainage storage system (Kido *et al*., 2007).

Alpine glacial basins are a significant source and storage area of sediment exposed by glacier retreat, suggesting that suspended sediments are generally associated with high sediment concentration during

*Correspondence to: Amit Kumar, Centre for Glaciology, Wadia Institute of Himalayan Geology, 33, GMS Road, Dehra Dun - 248 001, (Uttarakhand) India.
E-mail: amithydrocoin@gmail.com

snowmelt and rainfall events, resulting in the transfer of up to 70% at the gauging station (Orwin and Smart, 2004). Based on a global survey of sediment yield from 1358 drainage basins with their area ranging from 350 to 100 000 km^2, Jansson (1988) reported that within a particular climatic zone, where glaciers are active, sediment yield tends to be higher. Diurnal variation in suspended sediment from the high altitude region is controlled by the snow accumulation and meteorological condition (Singh *et al*., 2003); therefore, long-term observation of discharge and sediment load becomes necessary to understand subglacial sediment transfer processes. Research interests pertaining to sediment transport in higher Himalayan river basins have become important because of the huge hydropower potential in the region, and several studies have been carried out in recent times (Sharma *et al*., 1991; Hasnain and Thayyen, 1999; Bhutiyani, 2000; Kumar *et al*., 2002; Pandey *et al*., 2002; Jain *et al*., 2003; Owen *et al*., 2003; Bajracharaya *et al*., 2004; Singh *et al*., 2005; Ali and De Boer, 2006; Haritashya *et al*., 2006; Singh *et al*., 2008; Haritashya *et al*., 2010).

LOCATION AND GEOMORPHOLOGICAL SETTING OF STUDY BASIN

Dunagiri Glacier (30°33′20″N, 79°53′36″E) is a north-facing glacier, situated in Dunagiri Gad, a tributary of Dhauliganga river in Chamoli district of Uttarakhand [Figure 1 (a)]. Its identification number as per the glacier inventory of Himalaya is IN 5O 132 09044. It is a valley-type glacier occupying 17.9 km^2 area up to the gauging site [Figure 1 (b)]. The glacier camp is approachable by 18 km long foot/mule track from the nearest road head, Jumma. The elevation of glacier varies between 4200 near the snout and 5100 m at the head of the glacier. The length of the glacier is about 5.54 km. The morpho-geometry of Dunagiri Glacier is tabulated in Table I. The snout of the Dunagiri Glacier is marked from where the stream Dunagiri Gad emerges [Figure 2(a)]. The glacier is broad in the cirque region with several avalanche zones debauching in the cirque area. The glacier, in its present form, is bounded by left and right lateral moraines and a circular terminal moraine [(Figures 2 (b) and (d)]. A thick layer of supraglacial moraine or debris covers Dunagiri Glacier. It is dissected by several cerrac faces by which several small supraglacial lakes are bounded and have developed [Figure 2(c)].

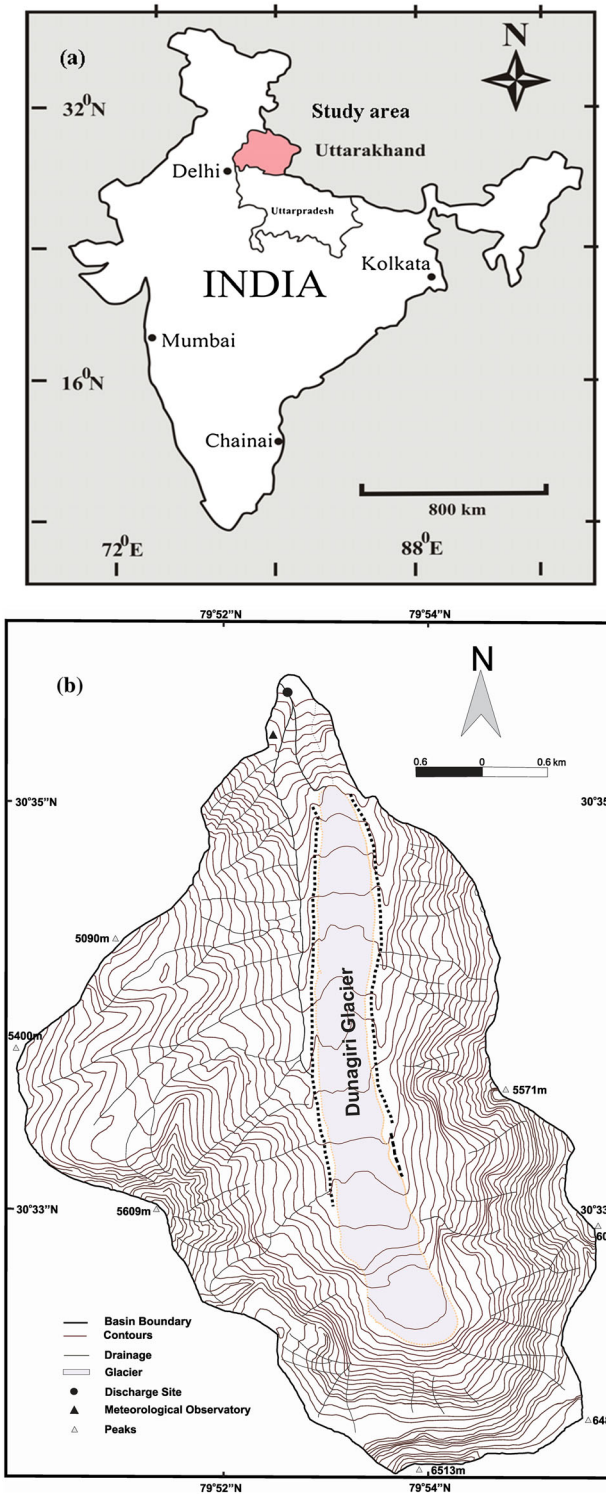

Figure 1. Locations of Uttarakhand and study area (a) and view of Dunagiri Glacier basin, up to the gauge site in Garhwal Himalaya (b)

METHODOLOGY

Collection of meteorological data

The importance of studying glaciers has attained considerable significance in context to the green house effect and global warming. Fluctuation in the air temperature may greatly influence the resultant runoff and sediment transport from the glaciers. Meteorological observations of parameters such as daily air temperature, rainfall, relative humidity and wind speed was carried out near the snout of Dunagiri Glacier during the years 1984–1989 using a conventional meteorological observatory. The frequency of data collection and instruments used are given in Table II. Other sources of data have also been utilised such as the records of Geological Survey of India (Srivastava and Swaroop, 1987, Srivastava *et al*., 1988; Srivastava and Swaroop, 1989; Swaroop and Gautam, 1990; Swaroop and Gautam, 1992).

Table I. Morpho-geometry of Dunagiri Glacier

S.No	Zone Area	Glacier Area	Source
1.	**Orientation**		Srivastava and Swaroop (1996)
1a)	Accumulation zone	NW	Raina and Srivastava (2008)
1b)	Ablation zone	N	
2.	**Elevation (m a.s.l)**		
2a)	Highest elevation	6489	
2b)	Lowest elevation	4250	
3.	**Mean elevation (m a.s.l)**		
3a)	Accumulation zone	5320	
3b)	Ablation zone	4580	
4.	Length of Glacier (km)	6.5	
5.	Mean width (km)	0.50	
6.	Total surface area (km^2)	4.39	
7.	Mean depth (km)	0.04	
8.	Total ice volume (km^3)	0.176	

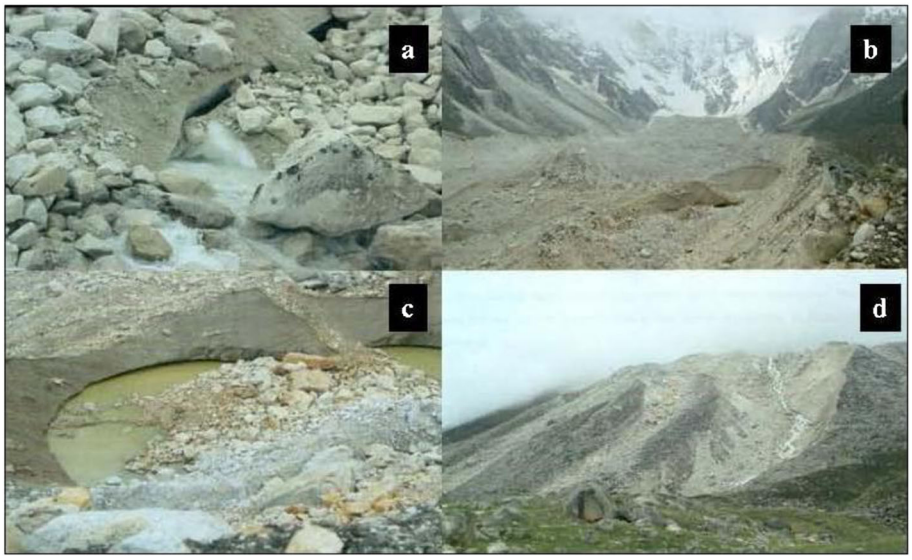

Figure 2. Locations of snout (a), lateral and terminal moraines (b) and (d), and supraglacial lakes (c) observed at Dunagiri Glacier

Table II. Meteorological instruments, observations on time interval near the snout of Dunagiri glacier

Instruments	Observations	Time of observations
Ordinary rain gauge	Rainfall	08:30, 11:30, 14:30 and 17:30 h
Maximum and Minimum Thermometers	Maximum and Minimum temperature	08:30 h and 17:30 h
Dry bulb and Wet bulb thermometers	Dry and Wet bulb temperatures	08:30, 11:30, 14:30 and 17:30 h
Hair hygrograph	Relative Humidity	08:30, 11:30, 14:30 and 17:30 h
Cup type anemometers	Wind speed	08:30, 11:30, 14:30 and 17:30 h
Wind Vane	Wind direction	08:30, 11:30, 14:30 and 17:30 h
Campbell stokes	Sunshine hours	06:00 h

Collection of discharge and suspended sediment data

For the estimation of sediment yield from the glacierised basins, discharge and suspended sediment measurements are required. During the ablation season, water levels were measured at the gauging site, and velocities were measured using the float method. Measurements were taken for the river cross sections at the gauging site regularly during the ablation season.

Discharge was computed by the velocity–area method utilising the water levels, velocities and the measured cross section of the stream. The discharge was very high, particularly during the peak melt period (July and August); therefore, the possibility of errors in the flow measurements, SSC/SSL estimation, is expected in the range of ±5% as discussed by Singh *et al*. (2006). For the determination of suspended sediment at the gauging site, water samples were taken in a clean bottle (500 ml) at an

interval of 4 h during the melt season (July–October). The samples were collected from the stream about mid-depth, filtered on site using ash-less filter paper. After weighing and drying, SSC for each sample was determined. Suspended sediment load (SSL) was determined by multiplying SSC with discharge and has been expressed in tonnes. The present study includes measurements for five ablation seasons (1984–1989).

RESULTS AND DISCUSSIONS

Meteorological data analysis

Climate of the central Himalayan region is considerably influenced by the south-west monsoon between May and September. The data collected from the rainfall (1984–1989) at the meteorological observatory near the snout of Dunagiri Glacier illustrates that out of all rainfall events, maximum rainfall occurs with an intensity of 43.5 mm and an average rainfall of 2.3 mm is experienced during the months of July, August and September [Figures 3 (a) and (b)]. Monthly rainfall exhibits significant variations from year to year especially during the monsoon months, and the total rainfall varied accordingly. The total rainfall (July to September) for the years 1984–1989 was computed to be 72.6, 185.5, 205.3, 127.1, 239.2 and 216.6 mm, respectively. The average monthly rainfall for July, August and September were 62.3, 75.5 and 47.0 mm, respectively [Figure 3 (b)].

The average daily maximum and minimum temperatures over the ablation season was 11.5°C and 6.1°C, with an average mean temperature of 8.8°C [Figure 3 (c)]. The distribution of temperature over the study period (1985–1989) shows that the mean monthly maximum temperatures for July to September were 12.4, 11.3 and 11.5°C, respectively, whereas mean monthly minimum temperatures for these months were 6.0, 6.3 and 5.5°C. The subsequent mean monthly temperatures for these months were computed to be 9.2, 8.8 and 8.5°C, respectively. The daily values of relative humidity ranged between 40.5 and 100%. Mean monthly relative humidity for July to September was 89, 90 and 78 % [Figure 3 (d)].

At high altitude, wind plays an important role in the transportation of moisture, formation of clouds, occurrence of precipitation and melting of glaciers. The daily mean wind speeds for July to September were 3.5, 3.8 and 5.5 km/h, respectively, and the average wind speed for the whole season was found to be 6.5 km/h. Maximum and minimum wind speeds observed were 13.2 and 0.3 km/h [Figure 3 (e)].

SSC and SSL

Distributions of daily mean SSC and discharge *versus* time for the Dunagiri Glacier are given in Figure 4 (a). Over the study period, daily mean SSC in the melt stream varied from 14.2 to 1987 mg/l. The SSC begins to increase with discharge from July onwards. However, the results indicate that discharge in the meltwater stream was less variable than SSC. Maximum daily mean SSCs observed in July, August and September were 712.2, 876.7 and 551.6 mg/l, respectively.

The mean monthly distribution of daily SSC is shown in Figure 4 (b). Mean concentrations of suspended sediment for July, August and September were observed to be 330, 365 and 200.3 mg/l, respectively. The mean daily SSC for the entire melt season was computed to be 229.01 mg/l. The variation in daily SSL and daily mean discharge during the ablation season is shown in Figure 5 (a). Daily SSL ranged between 12.3 and 608.1 tonnes/day at the gauging site. The monthly distribution of sediment load for different years is shown in Figure 5 (b). The average sediment load transported during the months of July, August and September were 57.3, 70.8 and 30.7 tonnes, respectively. The average total suspended load for the melt season was computed to be 45.6 tonnes. As compared with Dokriani Glacier in Garhwal Himalaya (Singh *et al*., 2003), results show that with SSC, maximum sediment loads from this glacierised basin occurred in August, followed by July. The higher peaks of SSL were associated with discharge through the entire melting seasons.

The percentage delivery of cumulative SSC in meltwater precedes that of corresponding discharge (Haritashya *et al*., 2006). To understand this delivery pattern of SSC and load, cumulative plots of discharge with SSC and load were made for each melt season [Figures 6 (a) and (b)]. It is observed that during the beginning of melt season (June–July), melt water discharge and suspended sediment correspond to each other, while in the peak melting season (August–September), the sediments are flushed out with high meltwater discharge. At the end of the melting season, the percentage of sediment decreases and tends to correspond to the meltwater discharge, except for the melt season of 1987, where the percentage delivery of SSC is reduced to that of discharge throughout the season. The percentage of sediment for the years 1984 and 1985 corresponds to the discharge throughout the season, whereas it is in advance of the corresponding discharge percentage for the years 1988 and 1989. The delivery pattern of SSL and discharge during the melt period remains similar; the percentage delivery of cumulative SSL is always in advance of the corresponding discharge during each melting season. From Figures 6 (a) and (b), it can be noted that there is a difference between the percentage delivery pattern of SSC and SSL with respect to discharge. The analysis suggests that the years 1988 and 1989 have the sediment concentration and load preceding discharge of the melt stream, i.e. 50% of cumulative SSC and SSL pass before that of discharge. The overall scenario for the study period suggests that cumulative SSC and SSL percentages pass before the corresponding discharge percentage in the peak melt season, and these show similar trends in the beginning and the end of the melt season.

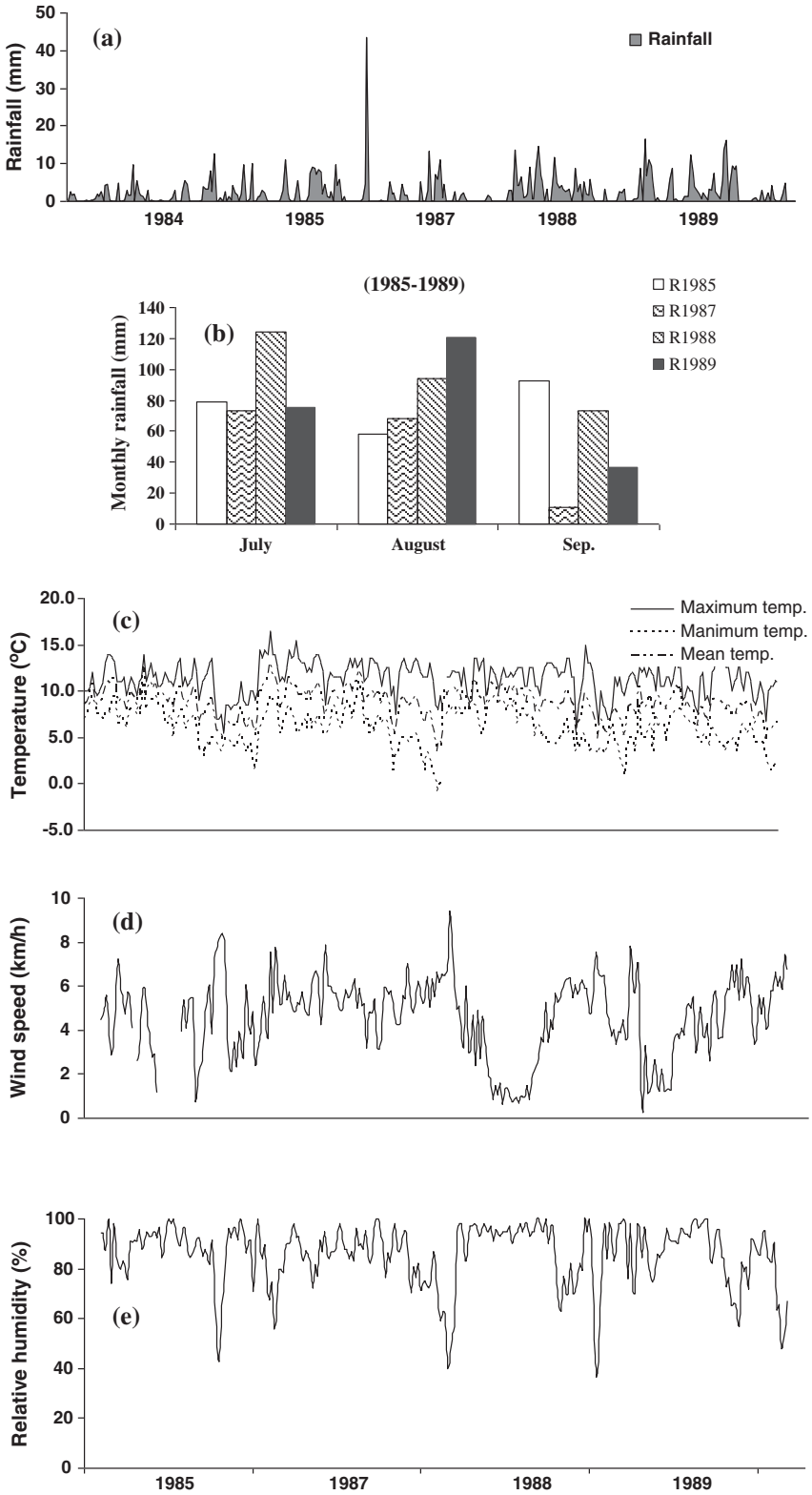

Figure 3. Meteorological observations at Dunagiri Glacier during the seasons (1984–1989): (a) daily rainfall (b) monthly rainfall (c) temperature (d) wind speed (e) relative humidity

Diurnal variation in SSC and SSL

Suspended sediment data were collected near the snout of the glacier at an interval of 4 h for the entire ablation season of 1987–1989. The percentage distribution of SSC corresponding to daytime (0800, 1200, 1600 h) and nighttime (2000, 2400, 0400 h) hours suggests that 53% of sediment concentration passes during the nighttime while 47% passes in the daytime; it means that on non-rainy days, or days having negligible rainfall in the study area during entire season, SSC varied significantly on the diurnal scale. It is observed that during the study period, the maximum SSC was at 2400 h followed by 2000 h, while minimum SSC was at 0800 h [Figure 7 (a)].

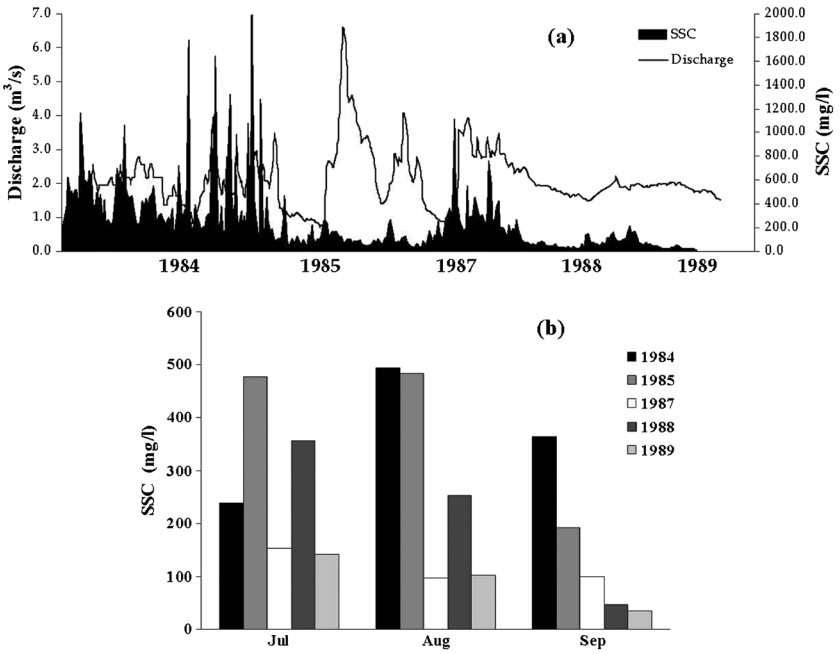

Figure 4. (a) Observed discharge and suspended sediment concentration in the Dunagiri Glacier melt stream during 1984 to 1989. (b) Mean monthly distribution of suspended sediment concentration observed at the Dunagiri Glacier gauging site for different years

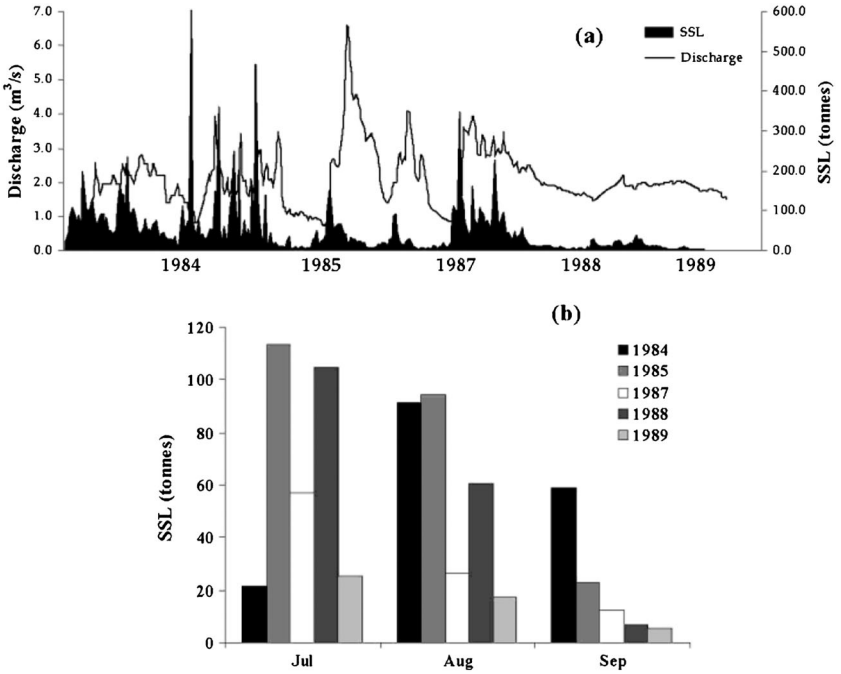

Figure 5. (a) Daily discharge and suspended sediment load (b) mean monthly distribution of suspended sediment load observed at the Dunagiri Glacier during 1984 to 1989

Maximum and minimum SSCs vary between 195.21 and 66.25 mg/l [Figure 7 (b)]. Similarly, sediment load was found to be higher in the night.

Assessments of sediment yield from Dunagiri Glacier and its comparison with other Himalayan glaciers

There are limited observations of sediment yield near the snout of Himalayan glaciers; most of the data available are of the lesser Himalayan region at greater distance from the glacier snout. Sediment yields for Dunagiri Glacier during different melt seasons from 1984 to 1989 were 259.1, 271.1, 265.6, 113.9, 203.8 and 40.8 tonnes/km^2, respectively, while the average yield for the period is 296.3 tonnes/km^2. Results show that there is a year to year variability in sediment yield, which could be due to several meteorological or hydrological factors (Collins, 1990; Hallet *et al*., 1996; Hodson *et al*., 1998; Srivastava *et al*., 1999). Time series plots [Figures 4 (a) and 5 (a)] for SSC and SSL of Dunagiri Glacier also suggest that sediment produced in a year may not flush out in the same year and may influence the sediment transport of

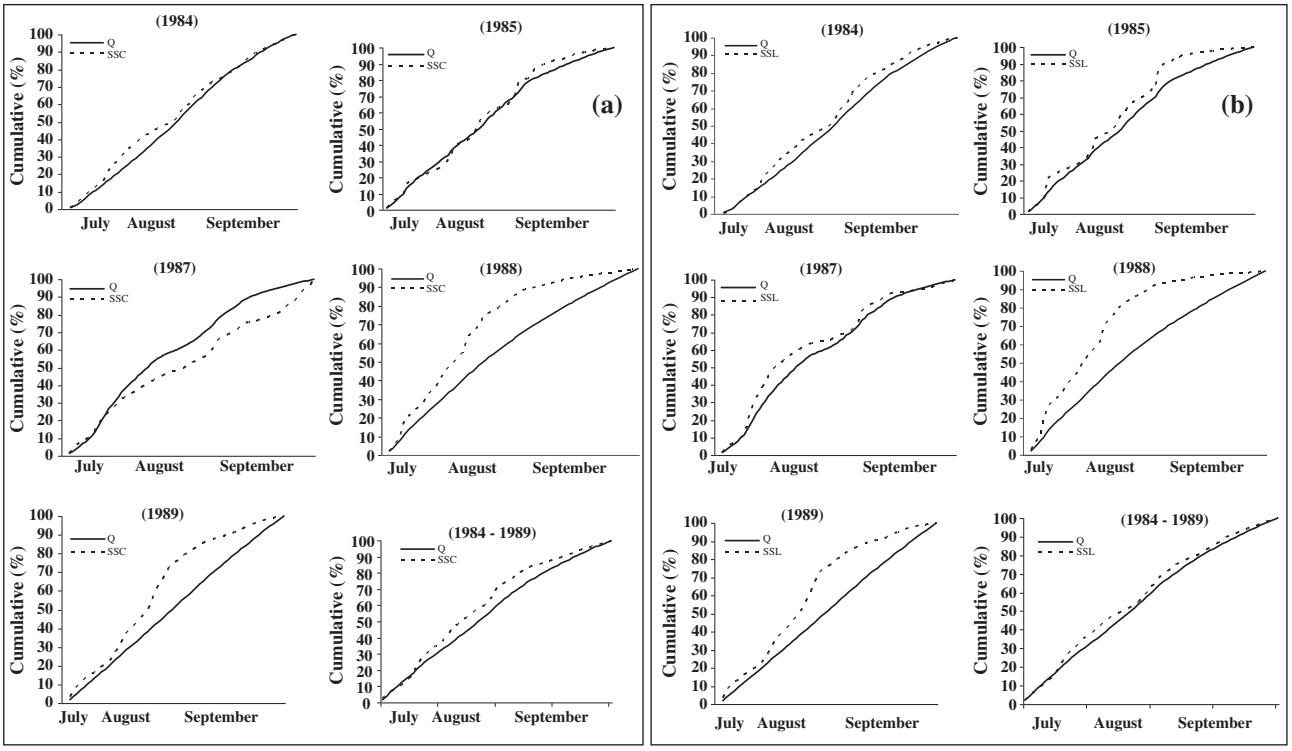

Figure 6. Distribution of cumulative percentage of total discharge *versus* SSC (a) and SSL (b) for the years 1984, 1985, 1987, 1988 and 1989

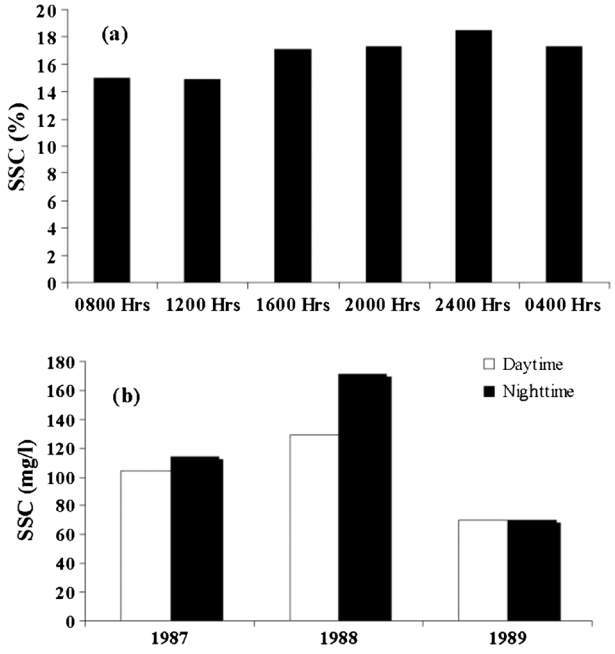

Figure 7. (a) Three hourly distribution of SSC from Dunagiri Glacier during the period (1987–1989) (b) Daytime and nighttime distribution of SSC from Dunagiri Glacier during the years (1987–1989)

succeeding years. It is also suggested that the largest sediment yields may not correspond to the years of high discharge (Haritashya *et al*., 2006).

Attempts were made to find out the relations, if any, of the suspended sediment transport by the glacier melt stream with the melt water discharge, the rainfall and the glaciated area, etc. The actuality is that sediment transfer from the glaciated regions of Himalaya is different with one glacier to others. On the basis of the available published data [(Table III (b)], it is suggested that there apparently exists no direct relationships between the suspended sediment transports with the melt-induced discharge, glacier area, glacier size, etc. Instead, this has a better relationship with the rainfall-induced discharge which in turn is again a subject of the intensity of storms. The major factors governing the SSL are the basin parameters, and geology of the terrain as the load transport by the streams is generated by the erosion of the basin.

In light of the sediment yield from Dunagiri glacier, we have compiled published case studies from the Himalayan region (Table IIIb). The average discharge volume draining from Himalayan glaciers were found different during the summer period, transported suspended sediment with different rates. Glaciers such as Tipra and Dokriani have higher discharge than Dunagiri glacier, but the Dunagiri glacier generates considerable amount of suspended sediment during the summer period (Figure 8 and Table IIIb).

Another major factor influencing the sediment yield is the amount of debris cover as debris is the major source of sediments. Hence, a glacier like Gangotri, which has a very thick cover of debris, will produce more sediment as compared to the less debris-covered glaciers such as Dokriani and Dunagiri. The other factor is the role of precipitation Dokriani glacier receives more than 1000 mm rainfall during summer season, whereas Gangotri receives ~259.5 mm rainfall during the summer

Table III. (a) Suspended sediment yield from Himalayan glaciers

Glaciers	Basin Area (km^2)	Glacierised Area (%)	Years	Average Sediment Yield (tonnes/km^2/yr)	Source
Dunagiri	17.9	14.3	1984–1989	296	Present study
Dokriani	16.33	59.2	1995–1998	2800	Singh *et al.* (2003)
Gangotri	556	51.4	2000–2003	4834	Haritashya *et al.* (2006)
Batura, Karakoram	650	60	1990	6086	Collins (1996)

Table III. (b) Mean daily suspended sediment load (SSL) from the Himalayan glaciers

Glaciers	Basin Area (km^2)	Glacierised Area(km^2)	Glacierised Area (%)	Mean SSL (tonnes)	Mean Discharge ($10^6\ m^3$)	Study periods (July-Sep)	Sources
Dunagiri	17.9	2.6	14.3	47.0	0.20	1984–1989	Present study
Gara	17.0	6.0	35	22.0	0.12	1974–1983	Raina (2009)
Shaune Garang	33.5	10.8	32.2	30.0	0.41	1981–1991	
Tipra Bank	41.6	13.1	31.5	40.0	0.67	1981–1988	Puri and Swaroop
Neh Nar	8.1	1.7	21	6.0	0.10	1975–1984	(1995)
Dokriani	16.3	9.7	59.2	446.6	0.45	1996–1998	Singh and Ramashastri (1999)
Gangotri	556.0	286	51.4	22 729	3.12	2000–2003	Singh *et al.* (2006)
Changme Khangpu	4.5	-	-	18.0	0.19	-	Puri (1999)

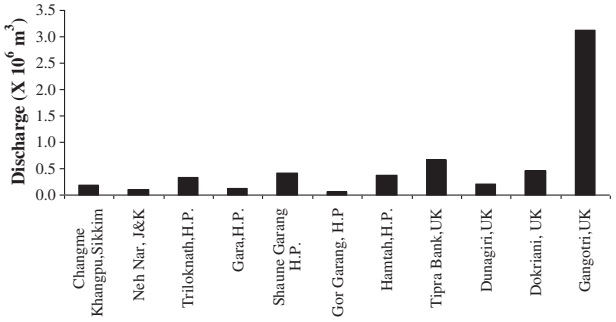

Figure 8. Mean discharge draining from Himalayan glaciers during different summer periods (July–Sep.) modified after Raina, 2009

season, which results in high sediment transfer in a single basin of the Bhagirathi river (Singh *et al.*, 2007). The process of sediment production and transfer by two different glaciers of a single basin is complex, and we suggest that further detailed studies of a number of glaciers in different regions of Himalaya should be carried out in order to establish any conclusion.

Suspended sediment rating curve for SSL estimation

The estimation of sediment volume from glacierised basins, carried by meltwater, is very important for many water resources projects. The prediction of river sediment concentration and load also constitutes an important issue in hydropower development. It is a well-known fact that all reservoirs are designed to have a volume known as 'the dead storage' to accommodate the sediment that will accumulates over a specified period; therefore, the prediction of river sediment load has an additional significance, especially if the sediment transport is by the glaciers. The relationship between SSL and discharge can be expressed in the following form:

$$SSL = aQ^b$$

or

$$\mathrm{Log}_{10}(SSL) = \mathrm{Log}_{10}(a) + b\mathrm{Log}_{10}Q,$$

where Q is the discharge and a and b are the estimated parameters. Log-transformed equations of SSC and SSL with the best linear fit curve for Himalayan glaciers are shown in Table IV. It is suggested that there is variability in both SSC and SSL with discharge for the whole melting season.

In Himalaya, limited number of attempts have been made to document the amount of sediment transported by a glacier to flow conditions such as meltwater discharge [Table III (a) and (b)]. Sometimes, simple sediment rating curve relationships (e.g. power law) may not adequately reproduce a good correlation with discharge of a stream, because sediment load carried out by a river is nonlinear or is a time-dependent factor. The present study shows that in 1988, the value of the correlation coefficient is 0.9, whereas it ranges between 0.6 and 0.7 for the years, 1984, 1986, 1987 and 1989 [Figures 9 (a) and (b)].

Inter-relationship between sediment concentration and mean temperature

In the Himalaya, air temperature is one of the controlling factors which influence snow and glacier melt. As we know that there is an association between sediment concentration and meltwater discharge, therefore, an attempt has been made to understand the relationship between SSC/SSL and mean monthly air temperatures. Results suggest a good correlation between mean monthly temperature with mean monthly SSC and mean monthly SSL for Dunagiri Glacier; an exponential relationship has been obtained for the mean monthly SSC

Table IV. Sediment rating curve developed for Dunagiri Glacier and other glaciers of Himalaya during ablation season

Glacier	Years	Rating Curve	R^2	Source
Dunagiri				
Seasons (July-Sep.)	(1984–1989)	$\text{Log}_{10}\ \text{SSC} = 1.610 + 1.7052 \times \text{Log}_{10}\text{Q}$	0.5	Present study
Seasons (July-Sep.)	(1984–1989)	$\text{Log}_{10}\ \text{SSL} = 1.6425 + 12\,699 \times \text{Log}_{10}\text{Q}$	0.5	
Siachen				
Seasons	(1987–1991)	$\text{Log}_{10}\ \text{SSL} = -6.4294 + 1.88 \times \text{Log}_{10}\text{Q}$	0.9	Bhutiyani (2000)
Gangotri				
Daily	(1999)	$\text{Log}_{10}\ \text{SSC} = -1.89 + 1.233 \times \text{Log}_{10}\text{Q}$	0.8	Kumar *et al.* (2002)
Daily	(2000)	$\text{Log}_{10}\ \text{SSC} = -2.196 + 1.453 \times \text{Log}_{10}\text{Q}$	0.6	
Gangotri				
Monthly (May-Oct)	(2000–2003)	$\text{Log}_{10}\ \text{SSC} = 1.3141 + 1.0862 \times \text{Log}_{10}\text{Q}$	0.9	Singh *et al.* (2006)
Daily (May-Oct)	(2000–2003)	$\text{Log}_{10}\ \text{SSC} = 0.9622 + 1.1953 \times \text{Log}_{10}\text{Q}$	0.5	
Dokriani				
Daily (June-Oct)	(1995–1998)	$\text{Log}_{10}\ \text{SSC} = 5.3958 + 0.652024 \times \text{Log}_{10}\text{Q}$	0.4	Singh *et al.* (2003)
Daily (June-Oct)	(1995–1998)	$\text{Log}_{10}\ \text{SSL} = 2.94664 + 1.65246 \times \text{Log}_{10}\text{Q}$	0.8	

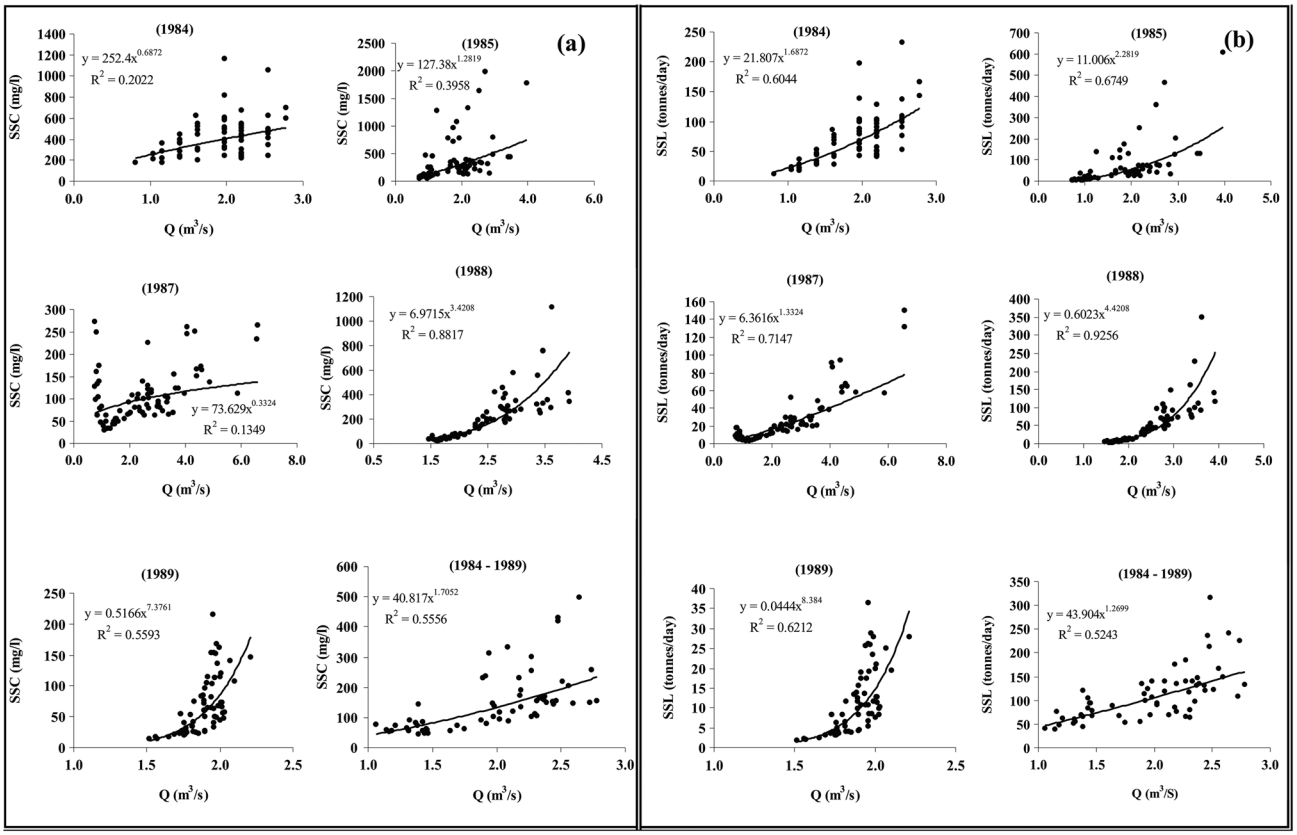

Figure 9. Relationships of SSC (a) and SSL (b) with discharge for the each melting season for the Dunagiri Glacier

and load (SSL) using the 1986–1989 data for Dunagiri Glacier [Figure 10].

It can be presented in the following equation, where T is the mean monthly air temperature and a and b are the estimated coefficients:

$$\text{SSC} = \text{a exp}\,(\text{bT})$$

The coefficient of determination between SSC and air temperature ($R^2 = 0.9$) suggests a strong relationship and dependency of sediment evacuation over the air temperature (Singh *et al.*, 2006). Thus, a small variation in the air temperature could give rise to exponential alteration in SSC, i.e. as the temperature rises over the ablation season, the SSC will increase exponentially. The sediment transport results obtained from the study show a lot of variations with respect to other studies in the Himalaya. The rise in global temperatures and the fact that most of the other studies have been carried out in the warmest decade might have been responsible for the large

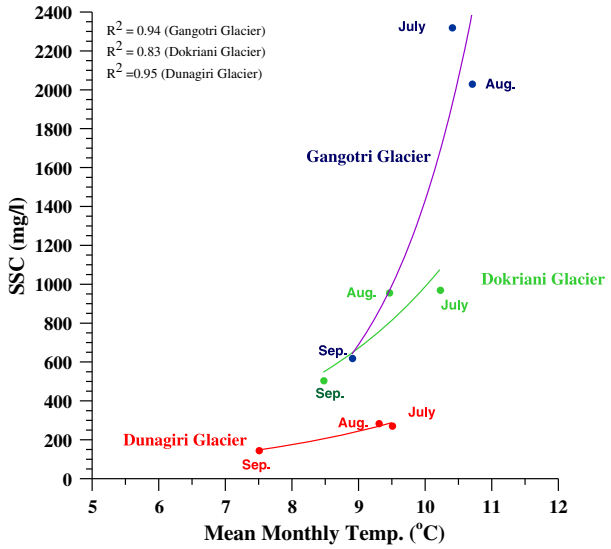

Figure 10. Relationship between mean monthly air temperature with SSC for the Dunagiri Glacier, 1985–1989 and its comparison with other Himalayan glaciers during ablation season (Singh and Ramashastri, 1999; Arora, 2009)

variations in the results obtained. Therefore, it will be appropriate to revisit the area and carry out further investigations in order to ascertain whether it is the effect of global warming or any other factor controlling the sediment delivery pattern in the region.

CONCLUSIONS

A limited number of studies have been made to establish a long-term data base on concentration and load from the Himalayan glaciers. Estimation of sediment transport in the streams by glaciers is very important for planning, designing and operating hydropower schemes in the Himalayan regions. SSL estimation is significant especially during the peak summer/monsoon period, as sediment inputs increase due to glacier melting and precipitation and cause damage of turbines in hydropower plant, and silting reduces the storage of reservoirs.

The present study deals with the estimation of SSC, load, yield and the development of rating curve for the estimation of suspended sediment for Dunagiri Glacier basin using data of six summer seasons. The source of sediment in the glacier melt water and processes associated with sediment generation, transport in the glacierised regions are discussed and compared with the previously published data.

Over the study period, daily mean SSC in the melt stream varied from 14.2 to 1987 mg/l, while daily SSL ranged between 12.3 and 608.1 tonnes/day. The average SSC and SSL for the months of July, August and September were 330, 365 and 200.3 mg/l and 57.28, 70.76 and 30.72 tonnes, respectively, which is equal to 158.76 tonnes for the season. The occurrence of peak pulse of sediment was associated with high discharge as rainstorms. Both sediment concentration and load are found to be highest in August followed by July. Sediment yield of Dunagiri Glacier basin is about 296.3 tonnes/km^2/yr. SSL shows a better correlation with discharge (R^2 =0.5 to 0.9) than the correlation between SSC and discharge (R^2 = 0.2 to 0.8). The sediment rating curve for all seasons was found to be less correlated for the SSC and SSL with discharge. However, on the other hand, the relationship between mean monthly SSC and SSL with air temperature was found to be well correlated exponentially (R^2 =0.9).

The study has shown that sediment yields from these basins of varying size can differ widely. Ultimately, it will be important to compare the sediment yield in these basins with others basins of varying size, physiography and land use history. Such an analysis would help to clarify how these factors interact to influence the dynamics of sediment storage and transfer. This will provide important understanding of basin processes that is needed to make well informed policy and management discussions.

The rise in global temperatures might be responsible for the large variations in the results obtained from different glaciers. There is a need to estimate sediment yields from all the glacierised basins of Himalaya to establish a long-term database by carrying out such studies for detailed investigation on concentration and load at high-resolution timescale. There is a direct impact and application of such studies on hydropower capacity of the Himalayan region, and therefore, sediment transport dynamics and yield of the basin must be taken into account while designing new reservoirs in the high altitude regions of Himalaya.

ACKNOWLEDGEMENTS

Authors offer their gratitude to Director General, Geological Survey of India for use of data (published and unpublished) in bringing out these results. The authors are very grateful to the Director, Wadia Institute of Himalayan Geology, Dehra Dun, for providing necessary facilities to carry out this study. We thank Dr. D.P Dobhal, Manish Mehta and Mr. Brijesh Badoni for their support during the work.

REFERENCES

Ali KF, De Boer DH. 2006. Spatial Patterns and variation of suspended sediment yield in the upper Indus river basin, northern Pakistan. *Journal of Hydrology* **334**: 368–387

Alley RB, Cuffey KM, Evenson EB, Strasser JC, Lawson DE, Larson GJ. 1997. How glaciers entrain and transport basal sediment: physical constraints. *Quaternary Science Review* **16**: 1017–1038.

Arora M. 2009. Seasonal characterisation of ablation, storage and drainage of melt runoff and simulation of streamflow for the Gangotri Glacier. Technical report submitted to Department of Science and Technology, Government of India.

Bajracharaya RM, Sharma S, Clemente R. 2004. Discharge and Sediment load of two streams in the mid-hill of Central Nepal. *Himalayan Journal of Science* **2**(3): 51–54.

Bhutiyani MR. 2000. Sediment load characteristics of a proglacial stream of Siachen Glacier and the erosion rate in Nubra valley in the Karakoram Himalayas, India. *Journal of Hydrology* **227**: 84–92.

Collins DN. 1979. Sediment concentration in meltwater as an indicator of erosion processes beneath an Alpine glacier. *Journal of Glaciology* **23**: 247–259.

Collins DN. 1990. Seasonal and annual variations of suspended sediment transport in meltwaters draining from an Alpine glacier. *International Association of Hydrological Sciences Publication* **193**: 439–446.

Collins DN. 1996. Sediment transport from glacierized basins in the Karakoram Mountains. Erosion and Sediment Yield: Global and Regional Perspectives Proceedings of the Exeter Symposium. *IAHS Publication* **236**: 85–96.

Collins DN. 1998. Suspended sediment flux in meltwaters draining from Batura glacier as an indicator of the rate of glacial erosion in the Karakoram mountains. *Quaternary Proceedings* **6**: 1–10.

Gurnell AM. 1995. Sediment yield from Alpine glacier basins. In *Sediment and Water Quality in River Catchments, Foster IDL, Gurnell AM, Webb BW (eds). Wiley: New York; 407–435.*

Gurnell AM, Hodson A, Clark MJ, Bogen J, Hagen JO, Tranter M. 1994. Water and sediment discharge from glacier basins: an arctic and alpine comparison. *IAHS Publication* **224**: 325–334.

Hallet B, Hunter L, Bogen J. 1996. Rates of erosion and sediment evacuation by glaciers: A review of field data and their implications. *Global and Planetary Changes* **12**: 213–235.

Harbor J, Warburton J. 1993. Relative rates of glacial and nonglacial erosion in alpine environments. *Arctic and Alpine Research* **25**: 1–7.

Haritashya UK, Singh P, Kumar N, Gupta RP. 2006. Suspended sediment from the Gangotri Glacier: quantification, variability and associations with discharge and air temperature. *Journal of Hydrology* **321**: 116–130.

Haritashya UK, Kumar A, Singh P. 2010. Particle size characteristics of suspended sediment transported in meltwater from the Gangotri Glacier, central Himalaya — An indicator of subglacial sediment evacuation. *Geomorphology* **122**(1-2): 140–152

Hasnain SI, Thayyen RJ. 1999. Discharge and suspended-sediment concentration of meltwaters, draining from the Dokriani Glacier, Garhwal Himalaya, India. *Journal of Hydrology* **218**: 191–198.

Hodgkins R. 1996. Seasonal trend in suspended sediment transport from an arctic glacier, and implications for drainage-system structure. *Annals of Glaciology* **22**: 147–151.

Hodson A, Ferguson RI. 1999. Fluvial suspended sediment transport from cold and warm-based glaciers in Svalbard. *Earth Surface Processes and Landforms* **24**: 957–974.

Hodson A, Gurnell A, Tranter M, Bogen J, Hagen JO, Clark M. 1998. Suspended sediment yield and transfer processes in a small High-Arctic glacier basin Svalbard. *Hydrological Processes* **12**: 73–86.

Iverson NR. 1995. Processes of glacial erosion. In *Glacial Environments: Modern Glacial Environments— Processes, Dynamics and Sediments, vol **1**, Menzies J (ed.). Butterworth-Heinemann: Oxford; 241–257.*

Jain SK, Singh P, Saraf AK, Seth SM. 2003. Estimation of sediment yield for a rain, snow and glacier fed river in the Western Himalayan region. *Water Resources Management* **17**: 377–393.

Jansson MB. 1988. A global survey of sediment yield. *Geografiska Annaler* **70A**: 81–98.

Kido D, Chikita KA, Hirayama K. 2007. Subglacial drainage system changes of the Gulkana Glacier, Alaska: discharge and sediment load observations and modelling. *Hydrological Processes* **21**(3): 399–410

Kumar K, Miral MS, Joshi V, Panda YS. 2002. Discharge and suspended sediment in the meltwater of Gangotri Glacier, Garhwal Himalaya, India. *Hydrological Sciences Journal* **47**(4): 611–619.

Lenzi MA, Mao L, Comiti F. 2006. Effective discharge for sediment transport in a mountain river: computational approaches and geomorphic effectiveness, *Journal of Hydrology* **326**: 257–276

Lewis T, Brown C, Hardy DR, Francus P, Bradley RS. 2005. An extreme sediment transfer event in a Canadian High Arctic stream. *Arctic, Antarctic, and Alpine Research* **37**: 477–482.

Milliman JD, Meade RH. 1983. Worldwide delivery of river sediments to the oceans. *Journal of Geology* **91**: 1–21.

Orwin JF, Smart CC. 2004. Short-term spatial and temporal patterns of suspended sediment transfer in proglacial channels, Small river glacier, Canada. *Hydrological Processes* **18**: 1521–1542.

Ostrem G. 1975. Sediment transport in glacial meltwater streams. In *Glaciofluvioal and Glaciolacurstine Sedimentation, Joping AV, McDonald BC (eds). Special Publication 23, Society of Economic Palaeontologist and Mineralogist: Tulsa Ok; 101–122.*

Owen L, Derbyshire E, Scott C. 2003. Contemporary sediment production and transfer in high-altitude glaciers. *Sedimentary Geology* **155**(1-2): 13–36.

Pandey SK, Singh AK, Hasnain SI. 2002. Grain-Size distribution, morphoscopy and element chemistry of suspended sediments of Pindari Glacier, Kumaon Himalaya, India. *Hydrological Sciences Journal* **2**: 213–226.

Puri VMK. 1999. Glaciohydrological and suspended sediment load studies in the melt water channel of Changme Khangpu Glacier, Mangam district, Sikkim. Symposium on Snow, Ice and Glaciers – Himalayan Prospective, Lucknow, 1.

Puri VMK, Swaroop S. 1995. Relationship of Glacierized area and summer mean daily discharge of glacier basins in Jhelum, Satluj and Alaknanda catchments in North western Himalaya. *Geological Survey of India, Special Publication* **21**(2): 315–319.

Raina VK. 2009. Himalayan Glaciers: A State-of-Art review of Glacial studies, Glacial Retreat and climate change. Ministry of Environment and Forest discussion paper.

Raina VK, Srivastava D. 2008. *Glacier Atlas of India. Geological Society of India: Bangalore.*

Schmidt K, Morch D. 2006. Sediment output and effective discharge in two small high mountain catchments in the Bavarian Alps, Germany. *Geomorphology* **80**: 131–145.

Sharma PD, Goel AK, Minnas RS. 1991. Water and sediment yields into the Satluj River from the High Himalaya. *Mountain Research Deveopment***11**(2): 87–100.

Singh P, Ramashastri KS. 1999. Temporal distribution of Dokriani Glacier melt runoff and its relationship with meteorological parameters. Technical report submitted to Department of Science and Technology, Government of India.

Singh P, Ramasastri KS, Kumar N, Bhatnagar NK. 2003. Suspended Sediment transport from the Dokriani Glacier in the Garhwal Himalayas. *Nordic Hydrology* **34**: 221–244.

Singh P, Haritashya UK, Ramasastri KS, Kumar N. 2005. Diurnal variations in discharge and suspended sediment concentration, including runoff-delaying characteristics, of the Gangotri Glacier in the Garhwal Himalayas. *Hydrological Processes* **19**: 1445–1457.

Singh P, Haritashya UK, Kumar N, Singh Y. 2006. Hydrological characteristics of Gangotri Glacier, Central Himalayas, India. *Journal of Hydrology* **327**(1-2): 55–67.

Singh P, Haritashya UK, Kumar N. 2007. Meteorological study for Gangotri Glacier and its comparison with other high altitude meteorological stations in Central Himalayan region. *Nordic Hydrology* **38**: 59–77.

Singh O, Sharma MC, Sarangi A, Singh P. 2008. Spatial and temporal variability of sediment and dissolved load from two alpine watersheds of the Lesser Himalayas. *Catena* **76**: 27–35.

Srivastava D, Swaroop S. 1987. Glaciological studies on Dunagiri Glacier, Chamoli district, Uttar Pradesh. Geological Survey of India, Records 122(8).

Srivastava D, Swaroop S. 1989. Mass balance variation, ablation pattern and surface fluctuations of Dungari Glacier, district Chamoli, Uttar Pradesh Proceedings of National Meet on Himalayan Glaciers DST New Delhi: 153–156.

Srivastava D, Swaroop S. 1996. Fluctuations of Dungari Glacier, district Chamoli, UP. *Geological Survey of India, Special Publication* **21**(2): 153–156.

Srivastava D, Swaroop S, Gautam CK. 1988. Glaciological studies on Dunagiri Glacier, Chamoli district, Uttar Pradesh. Geological Survey of India, Records 123(8).

Srivastava D, Swaroop S, Mukerji S, Gautam CK, Roy D. 1999. Suspended sediment yield and its variation in Dunagiri Glacier melt stream, Garhwal Himalaya. Abstract of the Symposium on Snow, Ice and Glaciers - A Himalayan perspective, Lucknow, 45.

Swaroop S, Gautam CK. 1990. Glaciological studies on Dunagiri Glacier, Chamoli district, Uttar Pradesh. Geological Survey of India, Records 124(8).

Swaroop S, Gautam CK. 1992. Glaciological studies on Dunagiri Glacier, Chamoli district, Uttar Pradesh. Geological Survey of India, Records 126(8).

Syvitski JPM. 2003. Supply and flux of sediment along hydrological pathways: research for the 21st century. *Global and Planetary Changes* **39**: 1–11.

Walling DE, Fang D. 2003. Recent trends in the suspended sediment loads of the World's rivers. *Global and Planetary Changes* **39**: 111–126.

Wenfeng D, Kateb HE. 2011. Annual discharge and sediment load variation in Jialing River during the past 50 year. *Journal of Mountain Science* **8**: 664–676.

Willis IC, Richards KS, Sharp MJ. 1996. Link between proglacial streams suspended sediment dynamics, glacier hydrology and glacier motion at Midtdalsbreen, Norway. *Hydrological Processes* **10**: 629–648.

Global and Planetary Change 75 (2011) 108–118

Contents lists available at ScienceDirect

Global and Planetary Change

journal homepage: www.elsevier.com/locate/gloplacha

Recent trends in sediment load of the tropical (Peninsular) river basins of India

Dileep K. Panda *, A. Kumar, S. Mohanty

Directorate of Water Management (ICAR), Chandrasekharpur, Bhubaneswar -751023, Orissa, India

ARTICLE INFO

Article history:
Received 28 May 2010
Accepted 28 October 2010
Available online 4 November 2010

Keywords:
tropical rivers
sediment loads
non-parametric trends
regional trends
droughts
anthropogenic activity

ABSTRACT

The tropical river basins of India are important because of the coastal ecosystem that they sustain and the densely populated economic zones that they serve. This study examines the recent trends in sediment load and also explores the influence of the climatic and human forcing mechanisms on the land–ocean fluvial systems. A large dataset comprised of the sediment time series of different timescale during the period 1986–87 to 2005–06 from 133 gauging stations spreading across tropical river basins of India was analyzed. Results indicate dramatic reductions in sediment load in the tropical river basins, which is beyond the fold of assignable natural variability. Around 88% (62%) of the total 133 gauging stations showed decline in sediment loads in the monsoon (non-monsoon) season. The significant downward trends outnumbered the corresponding upward trends in high proportions for both the seasons. Striking spatial coherence was observed among the significant trends, suggesting the presence of the cross-correlation among the sediment records. The regional trends, which account the spatial correlation, also indicated the widespread nature of the sediment declines. The rainfall, which is characterized by the non-significant decreasing trends and also frequent drought years, is the primary controller of the sediment loads for most of the river basins. It may be inferred that a little change in rainfall towards the deficit side leads to a significant reduction in sediment load. This is due to the diversion and storage of runoff to meet the manifold increases in water requirements for the agriculture and industry. Among the tropical rivers, the maximum reduction in sediment flux has taken place for the Normada River (-2.07×10^6 t/yr) due to the construction of dam. Although the sea level is rising, we speculate that the significant reduction in sediment loads may also have influenced the coastal erosion in recent years. The results of this study can be utilized for the sustainable management of the tropical river basins in the backdrop of a predicted erratic monsoon rainfall and the growing anthropogenic stresses.

1. Introduction

There is a growing body of evidence pertaining to the significant reduction in sediment supply to the global ocean. This is primarily due to the anthropogenic entrapments in dams and reservoirs, which has resulted in noticeable changes in the hydrological, geomorphological, ecological functioning of the river basins (Walling and Fang, 2003; Chakrapani, 2005; Syvitski et al., 2005). Reduction of sediment flux with consequent increases in coastal erosion appears to have serious implications as the coastal zones are economically vital and also densely populated. The rivers draining the Asian continent, which supply a substantial proportion of the global sediment flux and play an import role in the land–ocean linkages (Hu et al., 2001), have drawn considerable scientific attention in recent years due to the evident decreases in sediment flux. Major rivers of China such as the Yellow (Wang et al., 2007), the Yangtze (Zhang et al., 2009), the Pearl (Zhang et al., 2008), and the Mekong (Lu and Siew, 2006) exhibited substantial reduction in sediment supply. Winterwerp et al. (2005) noted serious coastal erosion in the Chao Phraya delta of Thailand, and they attributed this to the dam construction.

The Indian rivers, divided into two broad systems based on the morpho-tectonic difference, show sharp distinction in sediment supply; the Gangetic river system carries annual average sediment of 2390 t (tons)/km^2 from the highly erodible Himalayan range while the tropical (Peninsular) river system carries 216 t/km^2 (Milliman and Meade, 1983). The summer monsoon rainfall during June–September, which is nearly 80% of the annual rainfall, predominantly influences the streamflow, sediment transport and channel morphology of the tropical Indian rivers (Kale, 2002). In contrast, the Gangetic river system experiences a perennial flow regime due to the melting of the glaciers of the Himalayan Mountains during the non-monsoon period. This seasonality of flow in the tropical rivers has led to the construction of multi-purpose dams and reservoirs (Agrawal and Chak, 1991) in order to safeguard the flood prone deltaic region and also to supply water during the drought and non-monsoon period. Although damming the rivers has brought ample societal benefits of the burgeoning population in terms of addressing the water and

* Corresponding author. Tel.: +91 674 2300060; fax: +91 674 2301651.
E-mail address: dileeppanda@rediffmail.com (D.K. Panda).

0921-8181/$ – see front matter © 2010 Elsevier B.V. All rights reserved.
doi:10.1016/j.gloplacha.2010.10.012

energy crisis, the ecological consequences have received little scientific attention.

A recent study undertaken by the National Institute of Oceanography showed that 23% of the 5423 km mainland coastline of India experienced the coastal erosion. Using remote sensing imageries, Malini and Rao (2004) observed that the landward regression of the Godavari River basin led to evacuation of coastal establishments and loss of mangrove forest. They attributed this coastal erosion to the drastic reduction in sediment supply due the upstream reservoir construction. Further, Bobba (2002) reported the cases of seawater intrusion into the coastal aquifer of the basin. The Krishne River basin, the largest regulated river basin in term of dams and reservoirs in India, experienced coastal erosion due to the drastic reduction in streamflow and sediment flux (Bouwer et al., 2006; Biggs et al., 2007; Gamage and Smakhtin, 2009). Similarly, the upstream damming in the Normada River basin has resulted in significant reduction in sediment flux to the Arabian Sea (Gupta and Chakrapani, 2005). Syvitski et al. (2009) noted that the Mahanadi–Brahmani and Godavari basins were at greater risk to coastal erosion while the Krishna basin was in peril with high accelerated compaction among the major deltas of the world.

The global environmental change programs facilitated by the International Geosphere Biosphere Program (IGBP) Water Group, recommends that studies should delineate the increasing and decreasing sediment load due to human and/or climate change along the fluvial systems (Syvitski, 2003). Most of the studies on the sediment transport have used the time series data of the terminal gauging station or few stations at the mouth of river basin as they reflect the net flux to the global ocean. Nevertheless, there is a need to study the changes in sediment load across the river basin in order to understand the conflicting anthropogenic impacts in term of increases in soil erosion due to the deforestation and agriculture against the entrapments in dams (Syvitski, 2003). A major obstacle to assess the impacts of climate and anthropogenic activity on the global sediment system is the lack of reliable sediment monitoring time series (Dearing and Jones, 2003). In India, the sediment monitoring program with adequate spatial representation of the river basins commenced in the mid-1980s. However, some of the tropical rivers have relatively long time series for a few stations at the mouth of the river, and have also been used for the trend analysis (e.g. Malini and Rao, 2004; Gamage and Smakhtin, 2009).

Consistent with the IGBP Water Group recommendation and a noteworthy background scenario, this study aims (1) to identify and quantify the sediment load trends in the tropical river basins of India; (2) to explore the influence of the rainfall variability and human activity on the fluvial system. The sediment time series of different timescale during the period 1986–87 to 2005–06 from 133 gauging stations spreading across tropical river basins of India were used. The tropical rivers are important because of the economically viable region that they drain and the density of population that they serve. Although the Himalayan river system carries massive sediments, the rivers flow into the Indian Ocean at few points only. The tropical rivers, however, spread all along the coastline, and thus serve several wetland ecosystems. To address the paucity of long time series data, we used the non-parametric statistical methods for a more definitive assessment of the current trends in the land–ocean sediment transfer. To our knowledge, no previous studies have analyzed such a large dataset to depict the patterns of the sediment-load response across the river basins. In general, this study will provide critical inputs for the sound and sustainable management of the coastal zones in the context of the recent increases in the climatic extremes and the human interface. Additionally, the most ambitious mega project of India (i.e. the National River Linking Project (NRLP)) (Misra et al., 2007) can utilize the results of this study to earmark the environmental flow requirements while addressing the emerging water scarcity by transferring the water from the water-surplus basins.

2. An overview of the tropical river basins

The tropical river basins of India (Fig. 1) drain 43% of the total geographical area of 3.23×10^6 km^2, and they cover 46% of the total population of over one billion. Total average annual flow of the tropical rivers is 1869 km^3. Table 1 displays the diverse river basin characteristics of the tropical rivers reflecting the different geology, topography, rainfall, and demography. The Godavari River, the third largest river in term of drainage area after the Ganga and Brahmaputra Rivers of India, flows into the Bay of Bengal along with other major tropical rivers such as the Krishna, Mahanadi, Cauvery, Brahmani, and other east flowing rivers. The Normada is the largest tropical river that flows into the Arabian Sea followed by the Tapi, Mahi, and other west flowing rivers. In general, the sediment load of the tropical rivers draining the central Indian region (Godavari, Normada, Mahanadi, Brahmani, Tapi, Mahi) is much higher than that of the rivers draining the south Indian region (Krishna, Cauvery, Pennar of east flowing rivers).

The magnitude of the sediment flux from the tropical river basins is primary controlled by the rock formation of the basin and channel gradient. The hot tropical climate dominates the Godavari River basin. The western half of the basin is covered by the Deccan Trap, and contributes 50% of the annual sediment load. However, the hard rocks (39%) and sedimentary rock (13%) of the Godavari basin contribute 16% and 33% of the annual sediment load, respectively. The Krishna River basin having the predominant crystalline and basaltic rocks experiences a semi-arid climate. Although the Normada River is the fourth largest among the tropical rivers in term of the drainage area and annual streamflow, it is the second largest river in term of the sediment loads. The climate of the Normada River basin is humid tropical, and most parts of the basin have an elevation of ~500 m above the mean sea level. Further, the Deccan Trap is the major geological formation followed by the sedimentary rocks. The Mahanadi and Brahmani River basins, mostly covered by the Precambian rocks, experience a tropical monsoon climate with the substantial influence of the synoptic disturbances over the Bay of Bangal. Although the annual flow of the west flowing rivers is very high, the sediment load is much less in comparison to that of other river basins.

3. Data and methods

3.1. Data source

The Central Water Commission (CWC), an organization of the Ministry of Water Resources, Government of India, carries out the stream flow, sediment, and surface water quality monitoring activities. The datasets of the sediment loads employed in this study were obtained from the published reports of the CWC (CWC, 2006, 2007). Suspended sediment samples are collected from various marks along the cross-section of the river at the gauging stations using boats or specially designed instruments. The frequency of the sediment observation is daily in the monsoon season (June–September) and once in a week in the non-monsoon season (October–May), because the monsoon season supplies a large proportion of the annual sediment load. The data for the non-observed days is estimated based on the relationship between the observed sediment concentration and weighted mean discharge for the individual years. The analysis of suspended sediment samples provides information on the concentration of three separate size fractions, namely, coarse (>0.2 mm), medium (0.075–0.2 mm) and fine (<0.075 mm), respectively. The sediment concentration (gm/liter) for each group is recorded by passing the water sample through different mesh sieves of the British Standard Size. The discharge-weighted sediment load (t/day) for the river cross-section is obtained by multiplying the concentration by the discharge (m^3/second) on a particular day. These sediment loads are reported in the

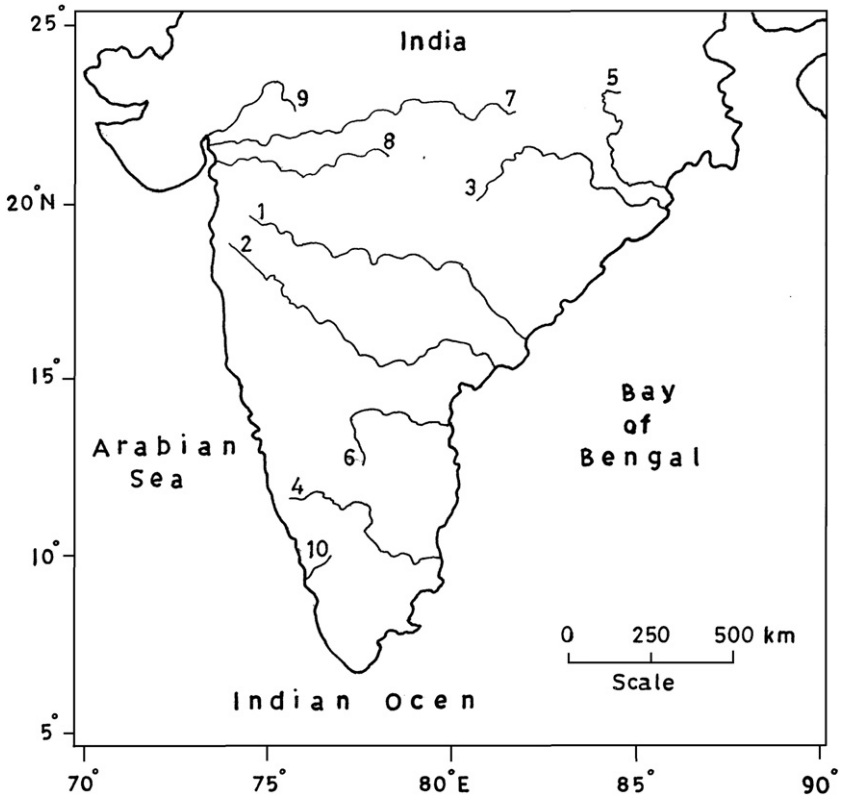

Fig. 1. Location of the tropical (Peninsular) rivers of India. The rivers (1) Godavari, (2) Krishna, (3) Mahanadi, (4) Cauvery, (5) Brahmani, and (6) Pennar (east flowing) drain to the Bay of Bengal whereas the (7) Normada, (8) Tapi, (9) Mahi, and (10) west flowing rivers flow into the Arabian Sea.

10-daily tables from each gauging station, which are subsequently added to find the monthly and seasonal sediment loads.

The complete datasets are not available to the public domain because of the existing water sharing conflicts among the river basin states. However, the CWC publishes the seasonal stream flow and sediment data in the 'Integrated Hydrological Data Book' after scrutinizing the uncertainty and heterogeneity of the data records. For the research purpose, the complete records can be obtained by following some official norms and regulations. The hydrological year starts at the beginning of June in a given year and extends up to the end of May in the subsequent year. The sediment records with a minimum 10 years of continuous time series were considered for this analysis as the non-parametric statistical tests can handle such short time series. Finally, we could assemble the monsoon and non-monsoon sediment loads of 133 gauging station available at different timescales from 1986–87 to 2005–06 for different river basins. This is the most recent dataset, which adequately represents the tropical river basins of India. The study periods and the number of monitoring sites of the river basins are presented in Table 1. To understand the relationship between the rainfall and the sediment flux, the basin-

Table 1
General information of the tropical river basins of India.

River basin	Latitude and longitude	Drainage area (10^5 km^2)	Length (km)	Annual flow (km^3)	Sediment load (10^6 t)	Annual rainfall (mm)	Population density per km^2	Storage capacity (km^3)	Study period	Gauging stations
Godavari	73° 26′ –83° 07′E to 16° 16′–22° 43′N	3.13	1465	110.5	170	1085	217	31.33	1986–87 to 2005–06	25
Krishna	73° 21′ –81° 09′E to 13° 07′–19° 25′N	2.59	1400	69.8	9.0	800	295	49.55	1986–87 to 2004–05	22
Mahanadi	80° 30′ –86° 50′E to 19° 20′–23° 35′N	1.42	851	66.9	30.7	1360	202	14.21	1993–94 to 2002–03	14
Brahmani	83° 52′ –87° 03′E to 20° 28′–23° 35′N	0.39	799	28.5	20.4	1200	204	5.25	1993–94 to 2002–03	8
Cauvery	78° 09′ –79° 27′E to 10° 00′–11° 18′N	0.87	800	21.4	1.5	800	389	8.87	1986–87 to 2002–03	11
East flowing (11 rivers)	77° 29′ –79° 59′E to 8° 12′–15° 56′N	0.82	–	22.76	–	800	722	3.03	1990–91 to 2003–04	5
Normada	72° 32′ –81° 45′E to 21° 20′–23° 45′N	0.99	1312	45.64	69.7	1180	187	23.6	1986–87 to 2002–03	14
Tapi	72° 38′ –78° 17′E to 20° 05′–22° 03′N	0.65	724	14.9	24.7	1000	245	10.26	1986–87 to 2001–02	8
Mahi	73° 13′ –74° 23′E to 23° 44′–24° 26′N	0.35	583	11.0	9.7	1000	324	4.98	1988–89 to 2001–02	9
West flowing (22 rivers)	73° 15′ –76° 51′E to 8° 43′–19° 10′N	0.30	–	200	–	2400	846	31	1990–91 to 2003–04	17

averaged annual rainfall datasets synthesized by the Indian Institute of Tropical Meteorology were used (Ranade et al., 2007).

3.2. Non-parametric tests

3.2.1. Site-specific trend assessment

The non-parametric Mann–Kendall (MK) statistical test (Mann, 1945; Kendall, 1975), a rank-based method, has been widely used in research studies to assess the monotone trend of hydro-climatic time series. The test is insensitive to the outliers and missing values, and also performs well over the competing class of parametric tests when the data are not normally distributed (Yue et al., 2002). The MK test statistics S is calculated as

$$S = \sum_{i=1}^{n-1} \sum_{j=i+1}^{n} \operatorname{sgn}\left(x_j - x_i\right) \tag{1}$$

where x is the data points at times i and j of a time series of length n. The sgn() is equal to $+1$ if x_j is greater than x_i, -1 if x_j is less than x_i, and 0 if x_j is equal to x_i. For the independent and identically distributed random variables with $n \geq 10$, the test statistics S is approximately normally distributed with the mean and variance given by

$$E(S) = 0, \tag{2}$$

and

$$\operatorname{Var}(S) = \frac{n(n-1)(2n+5) - \sum_{i=1}^{n} t_i(i)(i-1)(2i+5)}{18} \tag{3}$$

where t_i denotes the number of ties of extent i. The standardized test statistics Z is calculated as

$$Z = \begin{cases} \dfrac{S-1}{\sqrt{\operatorname{Var}(S)}} & \text{for} \quad S > 0 \\ 0 & \text{for} \quad S = 0 \\ \dfrac{S+1}{\sqrt{\operatorname{Var}(S)}} & \text{for} \quad S < 0 \end{cases} \tag{4}$$

Under the null hypothesis of no trend, the Z statistics follow a standard normal distribution. A positive value of Z indicates an upward trend, and a negative value of Z indicates a downward trend. The local significance levels (probability value p) of the Z statistics for each trend can be obtained by

$$p = 2[1 - \Phi(|Z|)] \tag{5}$$

where $\Phi()$ denotes the cumulative distribution function of a standard normal variate. For a very small p value, the trend denotes the systematic component of the data series and has not been caused by the random sampling. The existing trend is assessed to be statistically significant at the significance levels of 5% and 10%, if $p \leq 0.05$ and 0.1, respectively. To quantify the trend, the Kendall slope (β) was estimated by calculating the median of $(x_j - x_i)(j-i)^{-1}$ for all $i<j$.

Although the MK test is robust to the distribution and idiosyncrasies of data, the presence of serial correlation in the time series influences the trend results (Zhang et al., 2001). The positive serial correlation inflates the variance of the MK test statistics, leading to the increased probability of rejecting the null hypothesis of no trend (Von Storch, 1995). The presence of a negative autocorrelation, however, increases the probability of accepting the null hypothesis by reducing the variance of the MK test statistics. Incorporating the modified variance that minimizes the influence of serial correlation (Lettenmaier, 1976; Yue and Wang, 2002), the new MK test statistics can be defined as

$$Z^* = Z\left(\sqrt{\eta^s}\right)^{-1} \tag{6}$$

where $\eta^s = 1 + 2\frac{\rho_1^{n+1} - n\rho_1^2 + (n-1)\rho_1}{n(\rho_1 - 1)^2}$ for the lag-1 autocorrelation (ρ_1).

3.2.2. Regional trend assessment

We adopted the analytical method of assessing the trends at a regional scale proposed by Douglas et al. (2000), which finds the regional average of the MK test statistics as

$$\bar{S}_m = \sum_{k=1}^{m} S_k \tag{7}$$

where S_k is the MK test statistics for the at site k in a region with m sites. Without considering the spatial correlation (i.e. the cross correlation among the variables) of the region, the mean and variance of $\bar{S}_m$ are

$$E\left(\bar{S}_m\right) = 0 \tag{8}$$

$$\operatorname{Var}\left(\bar{S}_m\right) = m^{-1}\operatorname{Var}(S) \tag{9}$$

Subsequently, the standardized test statistics $\bar{Z}_m$ and the significance level p can be calculated using Eqs. (4) and (5). However, if the responses are cross-correlated, as is the case for most of the hydrologic variables, the variance of $\bar{S}_m$ in Eq. (9) becomes

$$\begin{aligned} \operatorname{Var}\left(\bar{S}_{mc}\right) &= \frac{1}{m^2}\left[\sum_{k=1}^{m} \operatorname{Var}(S_k) + 2\sum_{k=1}^{m-1}\sum_{l=1}^{m-k} \operatorname{Cov}(S_k, S_{k+l})\right] \\ &= \operatorname{Var}\left(\bar{S}_m\right)\left[1 + (m-1)\bar{\rho}_{k,k+l}\right] \end{aligned} \tag{10}$$

where $\bar{\rho}_{k,k+l} = \frac{2\sum_{k=1}^{m-1}\sum_{l=1}^{m-k}\rho_{k,k+l}}{m(m-1)}$ is the average cross-correlation for the region (Salas-La Cruz, 1972; Douglas et al., 2000). The standardized test statistics $\bar{Z}_{mc}$ can easily be derived as

$$\bar{Z}_{mc} = \bar{Z}_m\left(\sqrt{1 + (m-1)\bar{\rho}_{k,k+l}}\right)^{-1} \tag{11}$$

4. Results

We computed the location parameters of the sediment load at the last control stations of the basins in order to understand the seasonal and spatial differences. The last control stations at the mouth of the river (outlet) reflect the integrated response of the entire basin. Table 2 indicates that the monsoon season has contributed more than 90% of the annual sediment load. The presence of both the positive and negative Yule–Kendall skewness, which is a resistance measure of the shape of the distribution using the 25th percentile (Q_1), 50th percentile (Q_2), and 75th percentile (Q_3) as $(Q_1 - 2Q_2 + Q_3)/(Q_3 - Q_1)$ (Ferro et al., 2005), suggests the influence of the unusually high and low sediment loads, respectively. Fig. 2 shows that the variability in sediment load is consistent with the rainfall variability as evident from the direct correspondence between the annual sediment flux and the basin-averaged rainfall on an annual scale. Further, the LOWESS (i.e. locally weighted scatter-plot smooth) plots, a robust non-parametric procedure for estimating the regression surfaces (Cleveland and Devlin, 1988), indicate a clear decreasing pattern in both sediment flux and rainfall for most of the tropical river basins (Fig. 2).

Table 2
Summary statistics of the sediment flux (10^6 t) at the river basin outlets in the monsoon and non-monsoon seasons.

Basin	Period	Season	Mean	Standard deviation	Minimum	Q_1	Median	Q_3	Maximum	Yule–Kendall skewness
Godavari at Polavaram	1986–87 to 2005–06	Monsoon	57.72	38.36	19.40	28.42	46.71	72.26	158.58	0.17
		Non-monsoon	0.22	0.22	0.01	0.10	0.14	0.22	0.94	0.30
Krishna at Vijaywada	1986–87 to 2004–05	Monsoon	1.64	2.31	0.00	0.17	0.67	2.31	9.71	0.53
		Non-monsoon	0.10	0.16	0.00	0.01	0.04	0.13	0.65	0.65
Mahanadi at Tikarpara	1993–94 to 2002–03	Monsoon	11.78	15.79	1.99	3.03	6.98	10.53	55.05	−0.05
		Non-monsoon	0.67	0.38	0.07	0.38	0.73	0.95	1.24	−0.21
Brahmani at Jenapur	1993–94 to 2002–03	Monsoon	6.32	4.55	1.68	3.07	5.77	6.95	15.70	−0.39
		Non-monsoon	0.27	0.17	0.01	0.13	0.26	0.37	0.56	−0.07
Cauvery at Mausiri	1986–87 to 2002–03	Monsoon	0.25	0.25	0.03	0.13	0.16	0.38	0.88	0.73
		Non-monsoon	0.10	0.07	0.03	0.04	0.07	0.13	0.26	0.38
Pennar at Chennur	1990–91 to 2003–04	Monsoon	1.78	1.73	0.22	0.32	0.94	3.02	4.94	0.54
		Non-monsoon	0.05	0.10	0.00	0.01	0.03	0.04	0.40	−0.62
Normada at Garudeshwar	1986–87 to 2002–03	Monsoon	19.04	16.18	1.67	4.71	15.15	29.09	51.51	0.14
		Non-monsoon	0.06	0.07	0.00	0.02	0.03	0.06	0.20	0.60
Tapi at Sarankheda	1986–87 to 2001–02	Monsoon	19.38	14.85	4.69	7.65	18.23	22.75	54.79	−0.40
		Non-monsoon	0.08	0.21	0.00	0.00	0.00	0.03	0.83	0.83
Mahi at Khanpur	1988–89 to 2001–02	Monsoon	2.08	1.84	0.01	0.09	1.87	3.07	6.00	−0.20
		Non-monsoon	0.04	0.09	0.00	0.00	0.00	0.00	0.27	0.00
Nethravathi at Bantwal	1990–91 to 2003–04	Monsoon	1.19	0.72	0.32	0.65	1.16	1.52	2.77	−0.17
		Non-monsoon	0.01	0.02	0.00	0.01	0.01	0.02	0.06	0.45

Q_1: 25th percentile; Median (Q_2): 50th percentile; Q_3: 75th percentile.

The MK trend results summarized in Fig. 3 indicate that the decreases in sediment load predominate over the corresponding increases in high proportions for both the monsoon and non-monsoon seasons. Around 88% (62%) of the total 133 gauging stations across river basins showed declines in sediment load in the monsoon (non-monsoon) season. Around 27% and 42% of the total stations experienced significant decreases at the 0.05 and 0.1 levels, respectively in the monsoon season in comparison to that of 11% and 17% in the non-monsoon season. However, the significant increasing trends are infrequent or non-existent in the monsoon season (Fig. 3). It is interesting to note the presence of some upward trends in the non-monsoon season, although it contributes only a small fraction of annual sediment load. Fig. 4 presents the location maps of the significant trends ($p \leq 0.1$) in the monsoon and non-monsoon seasons. In general, an abundant decrease in sediment load was observed in the tropical river basins. The spatial distribution of the significant trends reveals noticeable patterns, suggesting the presence of cross-correlation among the sediment records. In the monsoon season, the significant downtrends have occurred across the tropical river basins with some concentration in the southern parts (Fig. 4a). In the non-monsoon season, however, the increasing trends are concentrated in the northwestern parts (i.e. Normada–Tapi–Mahi basin) (Fig. 4b). The decreasing trends tend to occur more towards the eastern parts (i.e. rivers flowing to the Bay of Bengal) of the study area.

Table 3 provides evidence that a major proportion of the total gauging stations showed significant decreasing trends for some of the major fluvial transporting river basins. In the Godavari basin, 16% and 36% of the total of 25 gauging stations experienced significant reduction at the 0.05 and 0.1 levels, respectively in the monsoon season. It is interesting to note that all the 22 gauging stations of the Mahanadi–Brahmani River basins showed decreases in sediment load in the monsoon and non-monsoon season. However, the significant reductions have occurred in 13% and 36% of the stations in the monsoon season at the 0.05 and 0.1 levels, respectively. The abundance of the decreases in sediment load is evident in the Krishna River basin as 59% and 73% of the 22 gauging stations exhibited significant reduction in the monsoon season at the 0.05 and 0.1 levels, respectively. In the Cauvery and east-flowing river basin, the decreases in sediment load were observed in 80% of the 16 gauging stations, although a few of them were statistically significant. Among the river basins flowing to the Arabian Sea, around 21% of the 14 gauging stations of the Normada River basin showed significant decreases in sediment load in the monsoon season at the 0.05 level. Further, the declining trend was observed in 87% of the 17 stations of the Tapi–Mahi River basin in the monsoon season. However, it is interesting to note the occurrence of increasing trends in more than 60% of the stations of these basins in the non-monsoon season. For the west-flowing rivers, around 94% of the 17 gauging stations were having decreasing trends in the monsoon season. However, the significant reduction in sediment load was observed in 29% and 52% of the stations at the 0.05 and 0.1 levels, respectively.

The spatial distribution of the significant trends ($p \leq 0.1$) shows the definite patterns even for the individual river basins, indicating the dependency among the sediment loads (Fig. 4). For example, most of significant decreases in sediment load are observed in the western catchments of the Godavari basin, whereas they are concentrated in the northwest parts of the Mahanadi–Brahmani River basins. Table 4 also indicates the presence of cross and serial correlations in sediment time series. In order to examine the overall pattern in a basin, we assessed the regional trend, which takes into account the spatial correlation among the sediment records. In the monsoon season, the regional trend in sediment load of the Godavari, Krishna, Mahanadi–Brahmani, Cauvery, Mahi, east-flowing and west-flowing river basins exhibited significant ($p \leq 0.1$) declining pattern (Table 4). This suggests the widespread (basin-wide) nature of the decreasing trends. However, the monsoon season reductions of the Tapi basin are localized as evident from the non-significant regional trends. In the non-monsoon season, it is interesting to note the basin-wide increases in sediment load of the Normada and Tapi River basins in contrast to an overall decreasing pattern for most of the basins. Based on the degree of correspondence with the rainfall (Table 5), we discuss the impacting factors of the sediment trends in the following sub-sections.

5. Discussion

5.1. Impacts of rainfall (climate) variability

The observed changes in sediment load of the tropical rivers of India reflect the impacts of the recent climate variability and its interaction with the anthropogenic activities as the study period represents the post-dam construction scenario for most of the river basins. The rainfall is the primary controller of the sediment flux to the adjacent ocean in the Godavari, Mahanadi, Cauvery, Brahmani, Tapi, Mahi River basins as evident from the significant correlations at the

0.05 level (Table 5). Table 1 also indicates that the storage capacity in dams and reservoirs in these basins is less in comparison to their annual flow, suggesting the minimal anthropogenic diversions. Further, the east-flowing and the west-flowing rivers are not impacted by the dams and reservoirs as evident from the low storage capacity and high annual rainfall (i.e. for the west-flowing rivers), although the sediment flux is weakly correlated with the rainfall for the Nethravathi and Pennar Rivers. The highest reduction in sediment flux (-1.40×10^6 t/yr) to the Bay of Bengal was observed at the last control station Polavaram of the Godavari River basin (Table 5). Further, the Mahanadi River experienced a significant ($p\leq0.1$) decreasing trend of -0.95×10^6 t/yr at the last control station Tikerpara, whereas the Brahmani River experienced a non-significant decreasing trend of -0.42×10^6 t/yr at Jenapur. The sediment flux to the Arabian ocean from the Tapi River also showed a significant ($p\leq0.1$) decreasing trend of -0.57×10^6 t/yr followed by a non-significant trend of -0.12×10^6 t/yr from the Mahi River at their respective outlets. In general, the decreases in sediment flux can be attributed to the decreases in rainfall. However, none of the river basin experienced significant decreasing trend in rainfall (Table 5). The LOWESS plots (Fig. 2) also suggest the substantial reduction in sediment flux in correspondence to a modest decreasing pattern in rainfall for most of the river basins.

Although several rivers show the basin-wide declines in sediment load, the trend of the sediment fluxes to the adjacent ocean from the outlets of these basins are not statistically significant. This suggests that the sediment fluxes are either stable or no apparent trend is observed due to the interaction of the changes in opposite direction.

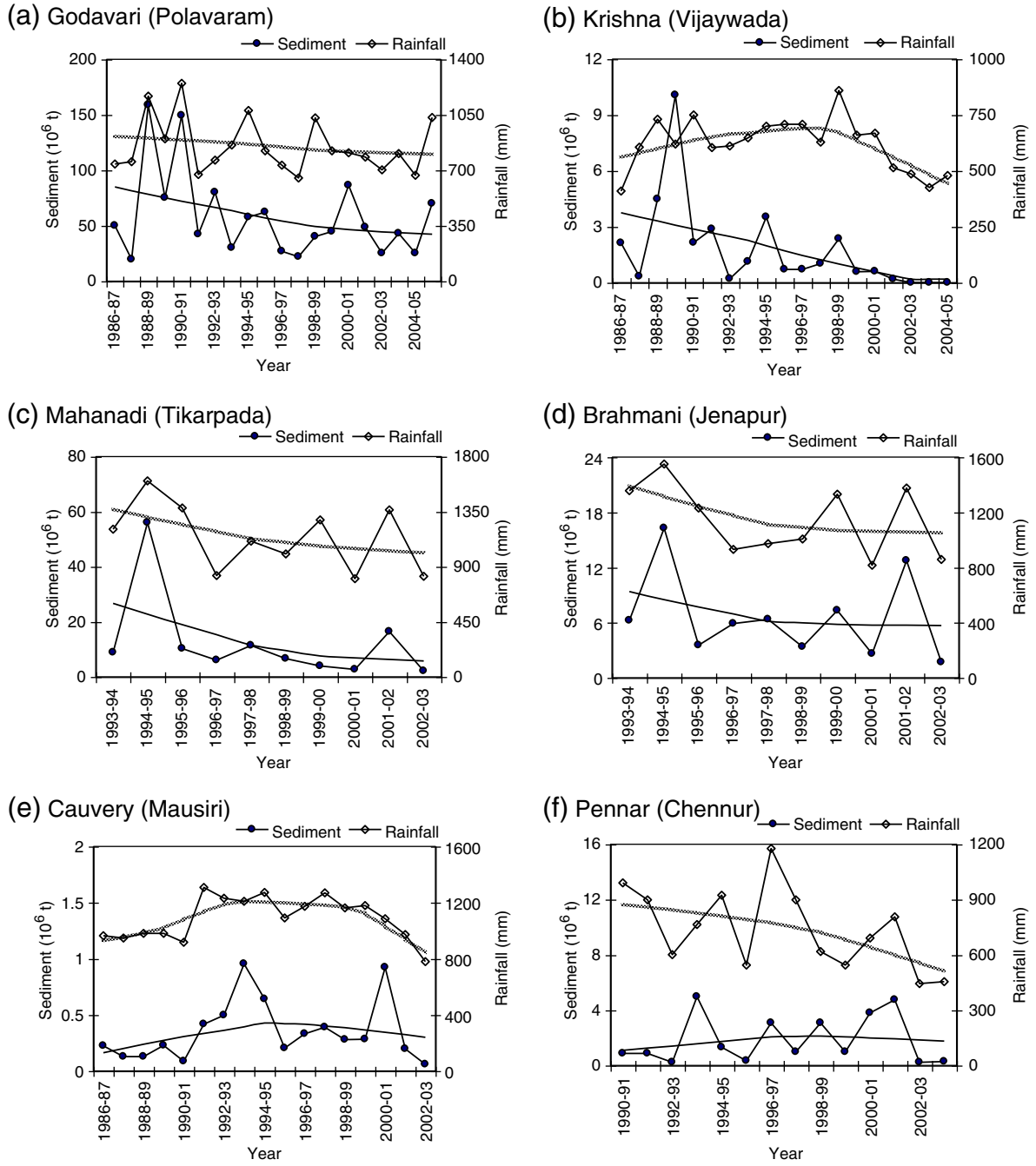

Fig. 2. Correspondence between the annual sediment flux (at the last gauging station) of the tropical rivers and the basin-averaged rainfall. The robust LOWESS plots (thick and thin lines) indicate a clear decreasing pattern in both sediment flux and rainfall for most of the river basins.

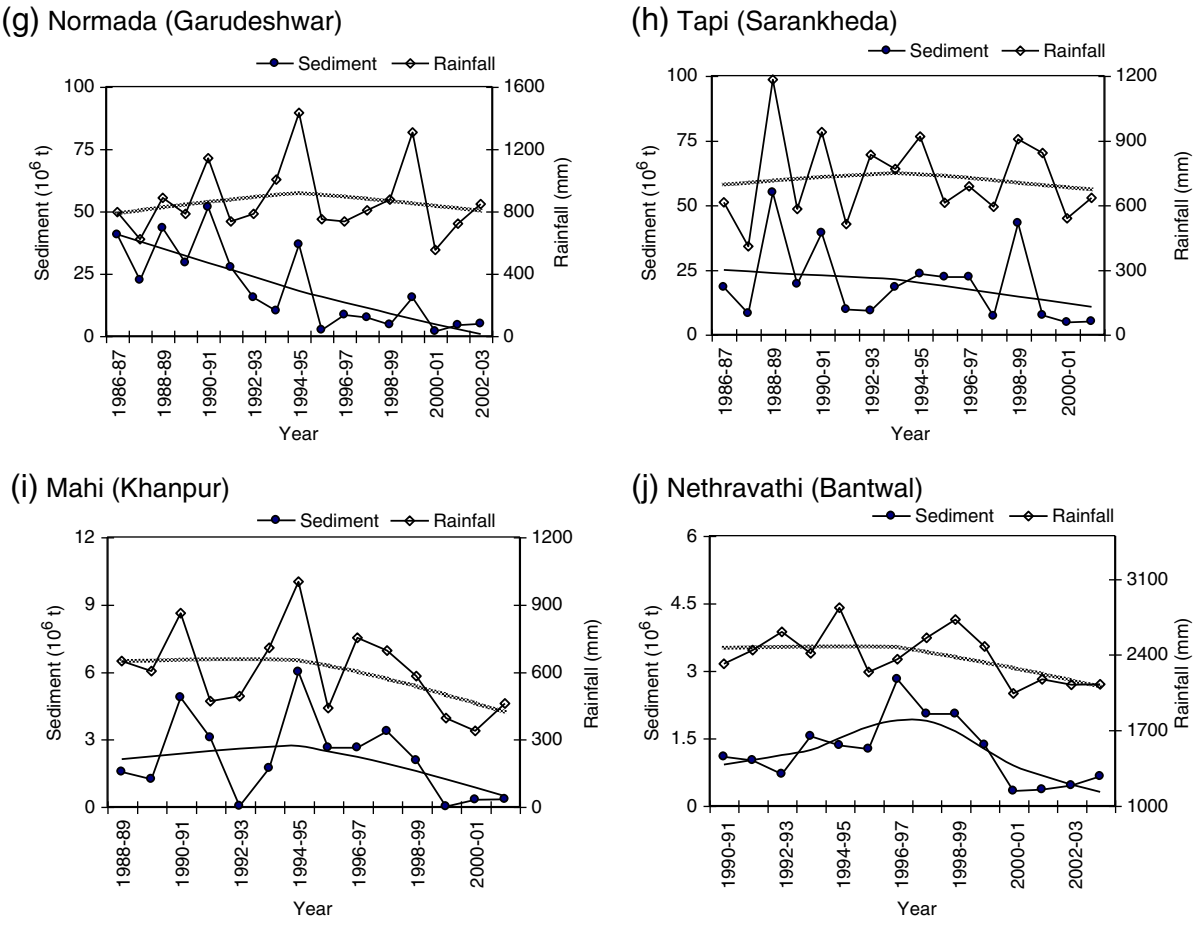

Fig. 2 (*continued*).

Fig. 2 provides evidence that the presence of high interannual variability in terms of the dry and wet years have obscured the underlying patterns in rainfall and sediment flux in most of the basins. The monsoon rainfall not only meets the water requirement of the predominant rain-fed agriculture in India but also recharges the groundwater that is used for irrigation and human consumption in a large scale. Therefore, a small deficit or skewed distribution in rainfall triggers the anthropogenic intervention in terms of the rainfall conservation and storage of runoff in the reservoirs in order to meet the amplified water demands in a drought year. For example, the Godavari River basin is heavily farmed with a cultivable area that encompasses 60% of the basin area, and two crops are grown due to assured irrigation from the major dams and reservoirs in the basin. It can be noticed that the sediment supply has reduced substantially during the drought years, which can be attributed to the diversion of the streamflow for the irrigation, drinking water and industrial water requirements. This is also the case for the Mahanadi, Brahmani, Cauvery, Mahi, and Tapi River basins. Therefore, the observed declines in sediment loads reflect the impacts of the frequent dry and deficit rainfall years and their interaction with the anthropogenic activities during the study periods.

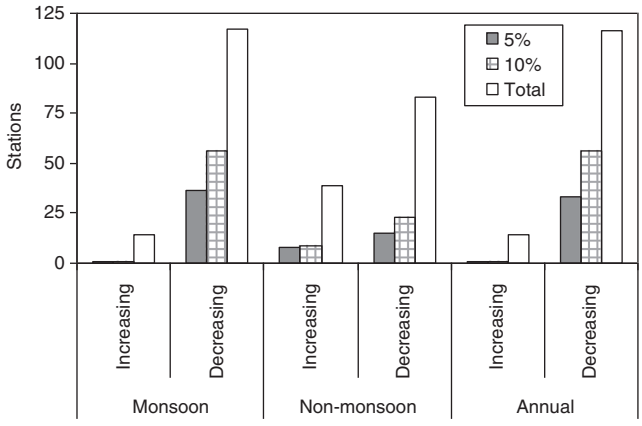

Fig. 3. The monsoon, non-monsoon, and annual sediment load trends in the tropical river basins of India. The gauging stations experiencing decreases in sediment load outnumber the corresponding increases in high proportions. The presence of significant decreasing trends at the 0.05 and 0.1 levels is also prominent irrespective of the seasons.

5.2. Impacts of dams and reservoirs

The Krishna and Normada River basins are highly regulated as a major portion of their annual runoff is earmarked for multifarious uses like electricity generation, irrigation and urban water supply (Table 1). Therefore, the correspondence between the rainfall and sediment load is critically distorted (Table 5). In the Krishna River basin, the stored water irrigates 3.2×10^4 km^2 area (i.e. 16% of the cultivable land) of the basin, and also produces 1947 MW of electricity annually. In addition, the reservoirs supply a large proportion of the drinking and domestic water requirements of the Hyderabad city with a population of 7 million. Therefore, the anthropogenic stresses appear to play a dominant role in comparison to the climate (rainfall) variability as the city population is increasing alarmingly along with the agriculture. The sediment flux at the outlet of the river basin (Vijaywada) to the Bay of Bengal exhibited significant ($p\leq0.05$) decreasing trend of -0.14×10^6 t/yr in

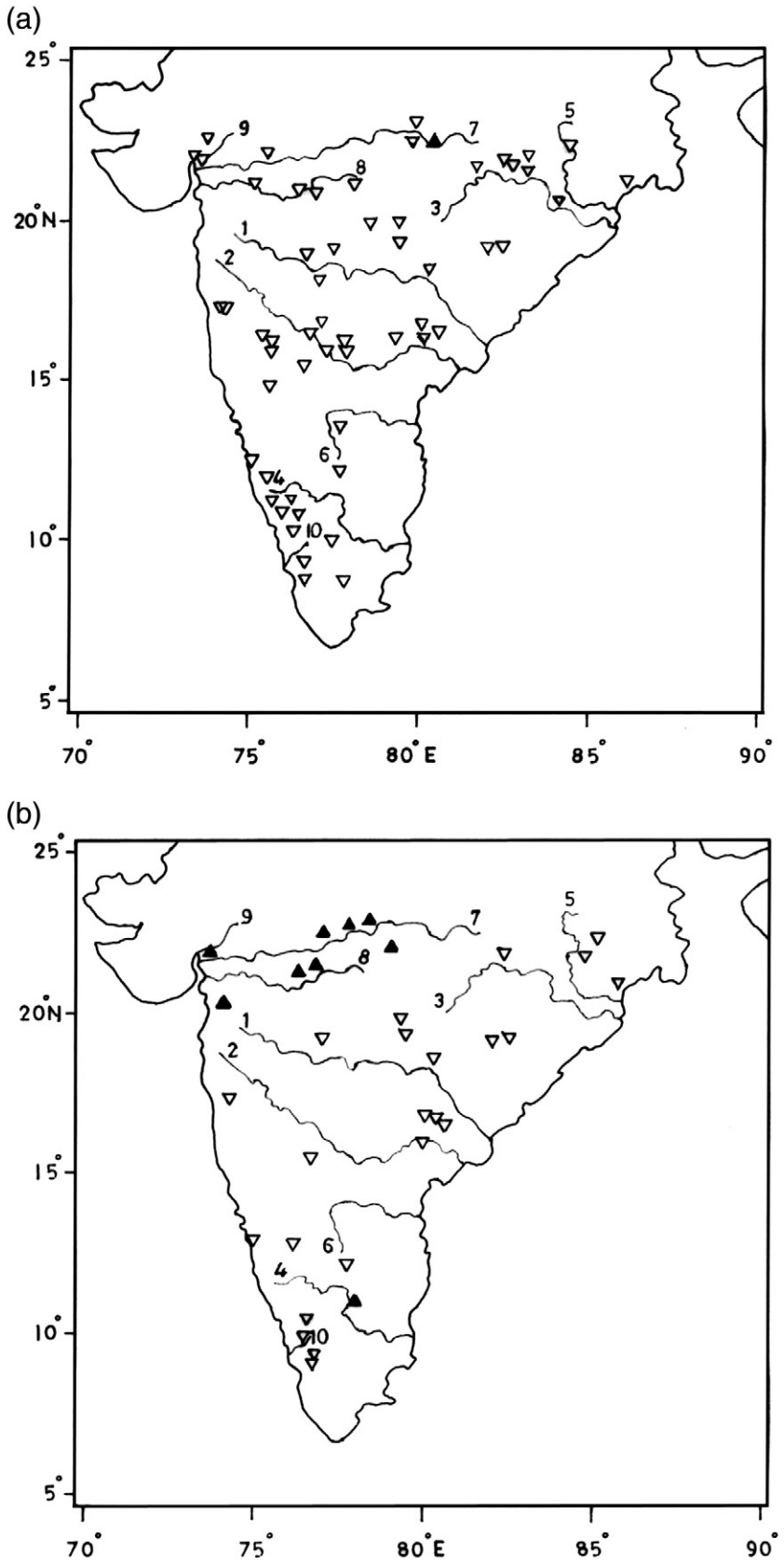

Fig. 4. Spatial distribution of the significant ($p \leq 0.1$) trends in sediment load of the tropical river basins of India in the (a) monsoon and (b) non-monsoon seasons. The occurrence of trends in group suggests the presence of the cross-correlation. The monsoon season, which supplies more than 90% of the annual sediment load, experiences widespread declining trends (inverted triangles) in sediment load. Few gauging stations show increases (filled triangle) in the non-monsoon season.

Table 3
Significant trends in sediment load of the tropical river basins in the monsoon and non-monsoon seasons.

River basin	Stations	Significance level	Monsoon		Non-monsoon	
			Increase	Decrease	Increase	Decrease
Godavari	25	0.05	0	4	0	4
		0.1	0	9	0	6
Krishna	22	0.05	0	13	0	5
		0.1	0	16	0	6
Mahanadi–Brahmani	22	0.05	0	3	0	1
		0.1	0	8	0	4
Cauvery and East-flowing	16	0.05	0	3	1	3
		0.1	0	4	1	3
Normada	14	0.05	1	3	5	0
		0.1	1	4	5	0
Tapi	8	0.05	0	3	1	0
		0.1	0	4	2	0
Mahi	9	0.05	0	2	1	0
		0.1	0	2	1	0
West-flowing	17	0.05	0	5	0	2
		0.1	0	9	0	4

correspondence to a non-significant decreasing trend in the basin rainfall. The recent decreases in sediment flux, which is even close to zero in some years, are due to the steady decrease in rainfall starting from the year 1997–98 (Fig. 2b). This suggests that almost all the rainfall of the basin have been captured in the reservoirs during the drought years. Further, it appears that much of the rainfall in the following normal year or even wet year have been used for refilling the deficits in the previous drought year.

The Normada River basin, which was supplying the largest volume of sediment to the Arabian Sea, experienced an abrupt reduction in sediment flux (Fig. 2g). The average sediment flux at the last control station Garudeshwar during the period 1986–87 to 1994–95 was 30.7×10^6 t/yr. This decreased to 6×10^6 t/yr during the period 1995–96 to 2002–03. Over the study period, the sediment supply dropped significantly ($p\leq0.05$) at the rate of -2.07×10^6 t/yr in correspondence to a non-significant rainfall trend. This trend can be attributed to the construction of the Sardar Sarovar dam, which entraps around 60–80% of the sediment loads (Gupta and Chakrapani, 2005). Although the Sardar Sarovar dam with a reservoir capacity of 3.7 km^3 renders immense societal benefits, the observed trend suggests that the anthropogenic regulation has altered the natural fluvial system of the basin. In general, coastal ecosystem develops resilience to the gradual trends in the hydroclimatic variables. However, the occurrence of abrupt reduction in streamflow and sediment flux can fundamentally alter the ecosystem function. The future research needs to examine the potential ecosystem responses to the abrupt shift in fluvial system. Further, the increases in sediment load in the non-monsoon season, which is widespread as evident from the regional trend results, could be attributed to the recent increases in the baseflow (Gupta and Chakrapani, 2007).

Table 4
Regional trends in sediment load with cross-correlation $\left(\bar{Z}_{mc}\right)$ in the tropical river basins.

Basin	Season	Gauging stations	Mean correlation		Regional trends	
			Serial	Cross	$\bar{Z}_{mc}$	p-value
Godavari	Monsoon	25	−0.04	0.22	−2.25	0.024
	Non-monsoon		−0.01	0.21	−1.96	0.050
Krishna	Monsoon	22	0.25	0.33	−3.98	0.000
	Non-monsoon		0.00	0.18	−1.97	0.050
Mahanadi–Brahmani	Monsoon	22	−0.20	0.44	−1.65	0.099
	Non-monsoon		−0.01	0.27	−1.84	0.066
Cauvery	Monsoon	11	0.15	0.23	−1.72	0.086
	Non-monsoon		0.07	0.12	−0.81	0.420
East-flowing	Monsoon	5	0.16	0.16	−2.91	0.004
	Non-monsoon		0.03	0.10	−2.76	0.006
Normada	Monsoon	17	−0.01	0.29	−1.17	0.241
	Non-monsoon		0.08	0.26	2.58	0.010
Tapi	Monsoon	8	−0.15	0.44	−1.35	0.178
	Non-monsoon		0.01	0.27	1.85	0.064
Mahi	Monsoon	9	0.06	0.34	−1.83	0.068
	Non-monsoon		0.05	0.06	1.36	0.174
West-flowing	Monsoon	17	0.26	0.40	−3.03	0.002
	Non-monsoon		−0.07	0.25	−1.56	0.119

5.3. Coastal erosion and the future scenario

The Fourth Assessment Report of the Intergovernmental Panel on Climate Change predicted that the global warming induced sea level rise along with the rainfall variability may aggravate the coastal ecosystem of the densely populated Asian river basins (Cruz et al., 2007). As the sea level is rising in the Indian coast (Unnikrishnan and Shankar, 2007), the simultaneous reduction in sediment supply observed in this study appears to have made the basins more vulnerable to the coastal erosion. The pristine Godavari River (i.e. the pre-dam scenario) was the 9th largest sediment transporting river on a global scale with an annual flux of 170×10^6 t. In the post-dam scenario, however, this has reduced substantially to 56.76×10^6 t during the period 1990–1998 (Malini and Rao, 2004). Our results reveal that the widespread declining tendency is still continuing in both the Godavari and Krishna River basins. Further, both the basins are prone to the global warming induced sea level rises (Rao et al., 2008). All these factors are likely to have caused the coastal erosion as evident from the loss of the mangrove vegetation and also the displacement of the human habitation (Malini and Rao, 2004; Gamage and Smakhtin, 2009).

Among the major deltas of the world, the Godavari and Krishna River basins are also identified as the basins at risk to coastal erosion where the reduced aggradation no longer keeps up with the local sea-level rise (Syvitski et al., 2009). With a reserve of 1060×10^6 t of hydrocarbon resources (Rao, 2001), both the basins are also prone to the coastal subsidence due to the extraction of natural gas from the underlying sediments. Further, the numerical modeling provides evidence of the sea water intrusion into the coastal aquifers due to the human activities and the sea-level changes (Bobba, 2002). Therefore, the proposed Polavaram project, which will link the water surplus Godavari River at Polavaram to the Krshna River at Vijaywada in order to meet the growing water requirements of the Krishna basin (GOI, Government of India, 1999b; Bharati et al., 2009), may further aggravate the coastal ecosystem.

The Mahanadi and Brahmani River basins are also highly vulnerable to the coastal erosion as both the deltas are sinking at a faster rate than that of the sea level rise (Syvitski et al., 2009). The long-term dataset available for the Tikarpara gauging station at the outlet of the Mahanadi River to the Bay of Bengal indicated a significant ($p\leq0.05$) declining sediment flux of -0.62×10^6 t/yr for the period 1980–81 to 2007–08. The observed reductions in sediment load appear to have exerted substantial influence on the coastal ecosystem as evident from the accelerated erosion hazards (Kumar et al., 2010). Further, the storms and severe cyclones developed over the northwest Bay of Bengal hit both the river basins more frequently than any other tropical river basins of India (Mascarenhas, 2004). This leads to frequent inundation of the coastal region. For example, the super cyclone in 1999 with a tidal surge of 8–10 m destroyed the coastal ecosystem, leading to serious socio-economic crisis (Mirza, 2003). In addition, the loss of the protective vegetation along the coast has made the deltas more vulnerable to even small tides. In the Brahmani River basin, the ENVIS (Environmental Information System of the wetland ecosystem of India) reported that the reduction in streamflow due to the construction of dam has increased the salinity of the Bhitarkanika estuary, leading to retardation of growth in mangrove forest. In order to sustain the ecological barrier, the requirement of the minimum environmental flow has also been highlighted.

Table 5
Trends in annual sediment load at the outlets of the tropical rivers and in basin rainfall.

River basin	Sediment trend			Rainfall trend			Correlation coefficient (r)
	Z^*	p-value	β (t/yr)	Z^*	p-value	β (mm/yr)	
Godavari at Polavaram	−1.02	0.308	−1.46	−0.91	0.363	−4.93	0.76[a]
Krishna at Vijaywada	−2.27	0.023	−0.14	−0.43	0.667	−6.49	0.25
Mahanadi at Tikarpara	−1.72	0.085	−0.95	−1.50	0.134	−42.61	0.72[a]
Cauvery at Mausiri	0.33	*0.371*	0.01	0.03	0.488	0.86	0.60[a]
Brahmani at Jenapur	−1.40	0.162	−0.42	−1.19	0.234	−43.42	0.80[a]
Penner (East flowing) at Chennur	0.26	0.397	0.01	−1.85	0.064	−30.12	0.31
Normada at Garudeshwar	−2.28	0.023	−2.07	−0.11	0.912	−0.60	0.40
Tapi at Sarankheda	−1.81	0.070	−0.57	−0.07	0.944	−1.17	0.76[a]
Mahi at Khanpur	−0.69	0.490	−0.12	−1.55	0.121	−20.30	0.81[a]
Nethravathi (West flowing) at Bantwal	−0.39	0.697	−0.05	−1.16	0.246	−26.78	0.52

[a] Significant correlation coefficient between the annual sediment load and the rainfall at the 0.05 level; β denotes the trend magnitude.

Besides the rainfall, the synoptic scale disturbances such as the storms and severe cyclones over the Indian Ocean influence both the sediment load and coastal erosion of the Indian coast. Particularly, the floods in the central India, which supply large proportion of the sediment loads in the Mahanadi–Brahmani, Godavari and Krishna River basins, are primarily associated with the cyclonic storms and depressions developed over the Bay of Bengal during the monsoon season. Recent studies show that the weakening of atmospheric dynamical parameters and the tropical easterly jet has led to the suppression of monsoon depressions in the Bay of Bengal (Dash et al., 2004). However, the rise in sea surface temperature (SST) has led to the intensification of the severe cyclonic storms in the non-monsoon seasons (Singh, 2007). We speculate the partial impacts of both the phenomenon in terms of the reduced sediment load in the monsoon season and the increased inundation in the non-monsoon season. The timing of the flood also influences the sediment loads as the high flows during the beginning of the monsoon season carry large quantity of sediment, and it decreases thereafter due to the vegetation cover. There are occasions when the Godavari has transported more than 7×10^6 t in a day (Vaithiyanathan et al., 1988). Further, when the adjacent ocean is stormy in term of the large tidal force, the high runoff creates new flood zones particularly in the flat deltas of the Godavari, Mahanadi and Brahmani Rivers due to the resistance of the Bay of Bengal to drain the flow, leading to the reduction in sediment flux.

Although there is limited evidence available regarding the impacts of climate change on the sediment loads (Walling and Fang, 2003), our result suggest that the anthropogenic control on the fluvial load is primarily associated with the climatic stresses. The early monsoon rainfall in India and the number of rainy days, which are important for the sediment loads, show decreasing trend (Ramesh and Goswami, 2007). Simultaneously, most of the tropical river basins have been experiencing an increasing trend in temperatures (Singh et al., 2008). The declining trends in sediment loads are spread across the river basins irrespective of the presence of dams and reservoirs. This indicates that the sediments are not only trapped in big reservoirs but also the soil and water conservation measures are intensified to meet the challenges of the frequent droughts. To support the burgeoning population and the developmental goals, the reservoirs that are in construction and those under consideration of construction will capture an additional annual flow of 184 km^3 (CWC, Central Water Commission (2006, 2007). The proposed interlinking of rivers will further reduce the sediment supply to the ocean (Misra et al., 2007). Therefore, the coastal erosion is likely to be accelerated if the current trends in sediment load continue well into the future.

6. Conclusions

Based on a large dataset comprised of the monsoon and non-monsoon sediment time series of different timescale during the period 1986–87 to 2005–06 from 133 gauging stations of the tropical river basins of India, this study investigated the trends in sediment load using the non-parametric statistical procedures. Results reveal clear signals of the declines in sediment load, which can be attributed to the impacts of the recent climate variability and its interaction with the anthropogenic activities. The observed variability in sediment load are in consistent with the rainfall variability for most of the basins (e.g. Godavari, Mahanadi, Cauvery, Brahmani, Tapi, Mahi River basins) as evident from the significant correlation coefficients. The sediment fluxes to the adjacent ocean at the outlets of these basins and also the average basin rainfall showed non-significant decreasing trends. This is due to the presence of high interannual variability in rainfall in terms of dry and wet years, which may have obscured the underlying patterns in both the rainfall and sediment flux. Highly regulated river basins such as the Krishna and Normada River basin exhibited significant reduction in sediment flux at the basin outlets, indicating the anthropogenic impacts in terms of stream flow storage and diversion. The Normada River, which was supplying the largest quantity of sediment to the Arabian Sea, also showed an abrupt reduction in sediment flux from 30.7×10^6 t/yr to 6×10^6 t/yr with an overall trend of -2.07×10^6 t/yr due to the construction of the Sardar Sarovar dam.

The observed significant downward trends in sediment load, which outnumbered the corresponding upward trends in high proportions for both the seasons, were found to spread across the river basins irrespective of the presence of the dams and reservoirs. This indicates that the sediments are not only trapped in big reservoirs but also the soil and water conservation measures are intensified to meet the challenges of the frequent droughts and the decreasing rainfall patterns. Strong spatial patterns were also observed among the significant trends, suggesting the presence of the cross-correlation among the sediment records. The regional trend, which accounts the spatial correlation, indicated significant reductions in the monsoon season for most of the river basins. This suggests the widespread nature of the sediment load declines. It may be assumed that the impacts of the proposed dams and the water conservation practices to deal with the climatic stresses will continue to reduce the sediment load. Based on our results, which identified the regions and locations of the significant reduction in sediment loads, policy measures need to be undertaken for the environmental flow requirements in order to safeguard the ecology and geomorphology of the densely populated deltas of India. Further research is required to quantify the relative contributions of different factors that influence the sediment trends and variability.

Acknowledgements

The authors would like thank the anonymous reviewers for their constructive comments and suggestions, which significantly improved the quality of the paper.

References

Agrawal, A., Chak, A., 1991. Floods, flood plains and environmental myths. State of India's Environment- A Citizens report. Centre for Science and Environment, New Delhi.

Bharati, L., Smakhtin, V.U., Anand, B.K., 2009. Modeling water supply and demand scenarios: the Godavari–Krishna inter-basin transfer, India. Water Policy 11, 140–153.

Biggs, T.W., Gaur, A., Scott, C.A., Thenkabail, Parthasaradhi, G.R., Gumma, M.K., Acharya, S., Turral, H., 2007. Closing of the Krishna basin: irrigation, streamflow depletion and macroscale hydrology. IWMI research report 111. International Water Management Institute, Srilanka.

Bobba, A.G., 2002. Numerical modeling of salt-water intrusion due to human activities and sea-level change in the Godavari Delta, India. Hydrological Sciences Journal 47, 67–80.

Bouwer, L.M., Aerts, J.C.J.H., Droogers, P., Dolman, A.J., 2006. Detecting long-term impacts from climate variability and increasing water consumption on runoff in the Krishna river basin (India). Hydrology and Earth System Sciences 10, 703–713.

Chakrapani, G.J., 2005. Factors controlling variations in river sediment loads. Current Science 88, 569–575.

Cleveland, W.S., Devlin, S.J., 1988. Locally weighted regression: an approach to regression analysis by local fitting. Journal of American Statistics Association 83, 596–610.

Cruz, R.V., Harasawa, H., Lal, M., Wu, S., Anokhin, Y., Punsalmaa, B., Honda, Y., Jafari, M., Li, C., Huu Ninh, N., 2007. Climate Change 2007: impacts, adaptation and vulnerability. In: Parry, M.L., Canziani, O.F., Palutikof, J.P., van der Linden, P.J., Hanson, C.E. (Eds.), Contribution of Working Group II to the Fourth Assessment Report of the Intergovernmental Panel on Climate Change. Cambridge University Press, Cambridge, UK.

CWC (Central Water Commission, 2006, 2007. Integrated Hydrological Data Book (Non-classified river basins). Hydrological data directorate. Central Water Commission, New Delhi.

Dash, S.K., Kumar, J.R., Shekhar, M.S., 2004. On the decreasing frequency of monsoon depressions over the Indian region. Current Science 86, 1404–1411.

Dearing, J.A., Jones, R.T., 2003. Coupling temporal and spatial dimensions of global sediment flux through lake and marine sediment records. Global and Planetary Change 39, 147–168.

Douglas, E.M., Vogel, R.M., Kroll, C.N., 2000. Trends in floods and low flows the United States: impact of spatial correlation. Journal of Hydrology 240, 90–105.

Ferro, C., Hannachi, A., Stephenson, D.B., 2005. Simple nonparametric techniques for exploring changing probability distribution of weather. Journal of Climate 18, 4344–4354.

Gamage, N., Smakhtin, V., 2009. Do river deltas in east India retreat? A case of the Krishna Delta. Geomorphology 103, 533–540.

GOI (Government of India), 1999b. The feasibility report of the Polavaram Vijayawada link. National Water Development Agency. Ministry of Water Resources, New Delhi.

Gupta, H., Chakrapani, G.J., 2005. Temporal and spatial variations in water flow and sediment load in Normada River Basin, India: natural and man-made factors. Environmental Geology 48, 579–589.

Gupta, H., Chakrapani, G.J., 2007. Temporal and spatial variations in water flow and sediment load in the Normada River. Current Science 92, 679–684.

Hu, D., Saito, Y., Kempe, S., 2001. Sediment and nutrient transport to the coastal zone. In: Galloway, J.N., Melillo, J.M. (Eds.), Asian Change in the Context of Global Climate Change: Impact of Natural and Anthropogenic Changes in Asia on Global Biochemical Cycles. : IGBP Publication Series, vol. 3. Cambridge Univ. Press, Cambridge, pp. 245–270.

Kale, V.S., 2002. Fluvial geomorphology of Indian rivers, an overview. Progress in Physical Geography 26, 400–433.

Kendall, M.G., 1975. Rank Correlation Methods. Griffin, London.

Kumar, T.S., Mahendra, R.S., Nayak, S., Radhakrishnan, K., Sahu, K.C., 2010. Coastal vulnerability assessment for Orissa state, east coast of India. Journal of Coastal Research 26, 523–534.

Lettenmaier, D.P., 1976. Detection of trend in water quality data from records with dependent observations. Water Resources Research 12, 1037–1046.

Lu, X.X., Siew, R.Y., 2006. Water discharge and sediment flux changes over the past decades in the lower Mekong River: possible impacts of the Chinese dams. Hydrology and Earth System Sciences 10, 181–195.

Malini, B.H., Rao, K.N., 2004. Coastal erosion and habitat loss along the Godavari delta front- a fall out of dam construction (?). Current Science 87, 1232–1236.

Mann, H.B., 1945. Nonparametric tests against trend. Econometrica 13, 245–259.

Mascarenhas, A., 2004. Oceanographic validity of buffer zones for the east coast of India: a hydrometeorological perspective. Current Science 86, 399–406.

Milliman, J.D., Meade, R.H., 1983. Worldwide delivery of river sediment to the oceans. Journal of Geology 101, 295–303.

Mirza, M.Q., 2003. Climate change and extreme weather events: can developing countries adapt? Climate Policy 3, 233–248.

Misra, A.K., Saxena, A., Yaduvanshi, M., Mashra, A., Bhadauriya, Y., Thakur, A., 2007. Proposed river-linking project of India: a boon or bane to nature. Environmental Geology 51, 1361–1376.

Ramesh, K.V., Goswami, P., 2007. Reduction in temporal and spatial extent of the Indian summer monsoon. Geophysical Research Letter 34, L23704. doi:10.1029/2007GL031613.

Ranade, A.A., Singh, N., Singh, H.N., Sontakke, N.A., 2007. Characteristics of hydrological wet season over different river basins of India. Indian Institute of Tropical Meteorology (IITM) research report (RR-119).

Rao, G.N., 2001. Sedimentation, stratigraphy, and petroleum potential of Krishna–Godavari basin, east coast of India. American Association of Petroleum Geologists Bulletin 85, 1623–1643.

Rao, K.N., Subraelu, P., Rao, T.V., Malini, B.H., Ratheesh, R., Bhattacharya, S., Rajawat, A.S., Ajai, 2008. Sea-level rise and coastal vulnerability: an assessment of Andhra Pradesh coast, India through remote sensing and GIS. Journal of Coastal Conservation 12, 195–207.

Salas-La Cruz, J.D., 1972. Information content of the regional mean. Proceedings of the International Symposium on Uncertainties in Hydrologic and Water Resources System, vol. 2. University of Arizona, Tucson. December 11-14.

Singh, O.P., 2007. Long-term trends in the frequency of severe cyclones of Bay of Bengal: observations and simulations. Mausam 58, 59–66.

Singh, P., Kumar, V., Thomas, T., Arora, M., 2008. Basin-wide assessment of temperature trends in northwest and central India. Hydrological Sciences Journal 53, 421–433.

Syvitski, J.P.M., 2003. Supply and flux of sediment along hydrological pathways: research for the 21st century. Global and Planetary Change 39, 1–11.

Syvitski, J.P.M., Vörösmarty, C.J., Kettner, A.J., Green, P., 2005. Impact of humans on the flux of terrestrial sediment to the global coastal ocean. Science 208, 376–380.

Syvitski, J.P.M., Kettner, A.J., Overeem, I., Hutton, E.W.H., Hannon, M.T., Brakenridge, G. R., Day, J., Vörösmarty, C., Saito, Y., Giosan, L., Nichlls, R.J., 2009. Sinking deltas due to human activities. Nature Geoscience. doi:10.1038/NGEO629.

Unnikrishnan, A.S., Shankar, D., 2007. Are sea-level-rise trends along the coasts of the north Indian Ocean consistent with global estimates? Global and Planetary Change 57, 301–307.

Vaithiyanathan, P., Ramanathan, A.L., Subramanian, V., 1988. Erosion, transport and deposition of sediments by the tropical rivers of India. Proceedings of the Porto Alegre Symposium, IAHS Publication no. 174, pp. 561–574.

Von Storch, H., 1995. Misuses of statistical analysis in climate research. In: Von Storch, H., Naverra, A. (Eds.), Analysis of Climate Variability: Applications of Statistical Techniques. Springer-Verlag, Berlin, pp. 11–26.

Walling, D.E., Fang, D., 2003. Recent trends in the suspended sediment loads of the world's rivers. Global and Planetary Change 39, 111–126.

Wang, H.J., Yang, Z.S., Saito, Y., Liu, J.P., Sun, X.X., Wang, Y., 2007. Stepwise decrease of the Huanghe (Yellow River) sediment load (1950–2005): impacts of climate change and human activities. Global and Planetary Change 57, 331–354.

Winterwerp, J.C., Borst, W.G., de Vries, M.B., 2005. Pilot study on the erosion and rehabilitation of a mangrove mud coast. Journal of Coastal Research 21, 223–230.

Yue, S., Wang, C.Y., 2002. Regional streamflow trend detection with consideration of both temporal and spatial correlation. International Journal of Climatology 22, 933–946.

Yue, S., Pilon, P., Cavadias, G., 2002. Power of the Mann–Kendall and Spearman's rho tests for detecting monotonic trends in hydrological series. Journal of Hydrology 259, 254–271.

Zhang, X., Harvey, K.D., Hogg, W.D., Yuzyk, T.R., 2001. Trends in Canadian streamflow. Water Resources Research 37, 987–998.

Zhang, S., Lu, X.X., Higgitt, D.L., Chen, C.A., Han, J., Sun, H., 2008. Recent changes in the water discharge and sediment load in the Zhujiang (Pearl River) basin, China. Global and Planetary Change 60, 365–380.

Zhang, Q., Xu, C.-Y., Singh, V.P., Yang, T., 2009. Multiscale variability of sediment load and streamflow of the lower Yangtze River basin: possible causes and implications. Journal of Hydrology 368, 96–104.